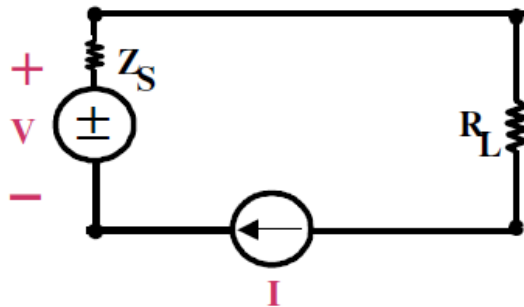




# Radiofrequency Power Measurement

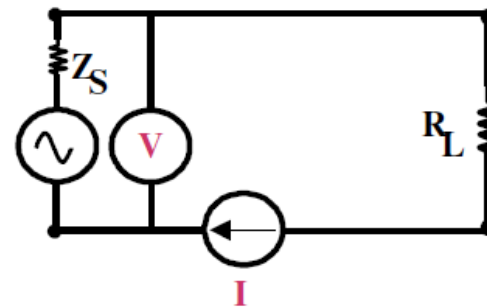
# Why not measure voltage?

DC



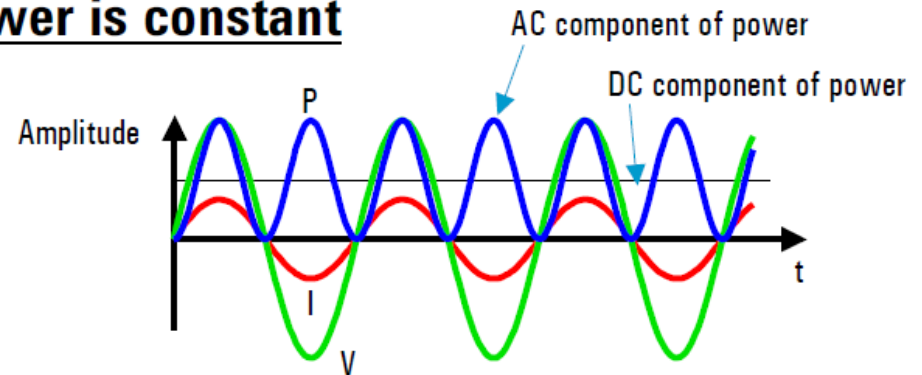
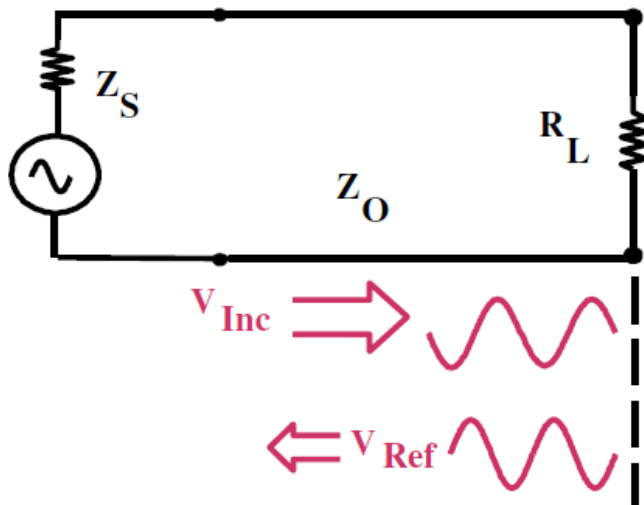
$$P = IV = V^2/R$$

Low Frequency



High Frequency

- **I** and **V** vary with position
- **Power is constant**



# Units and definitions

- Power = energy transferred per unit time
- Basic power unit is the watt (W)
  - $1 \text{ W} = 1 \text{ A} \times 1 \text{ V}$
- A logarithmic (decibel) scale is often used to compare two power levels
  - **Relative** power in decibels (dB) =  $10 \log(P_2/P_1)$
- **Absolute** power is expressed by assigning a reference level to  $P_1$ 
  - Power (dBm) =  $10 \log(P/1 \text{ mW})$

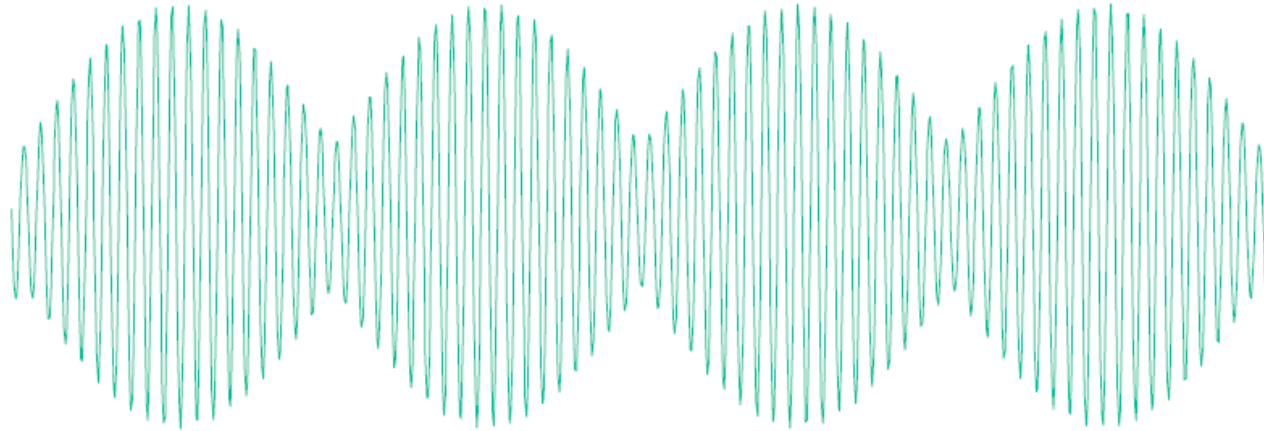
Instantaneous power  $p(t) = v(t)i(t)$

DC:  $i(t) = I; v(t) = V \rightarrow P = VI = V^2/R = I^2R$

AC:  $P = \frac{1}{\tau} \int_t^{t+\tau} v(t)i(t)dt = VI \cos \varphi$

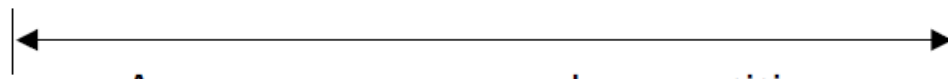
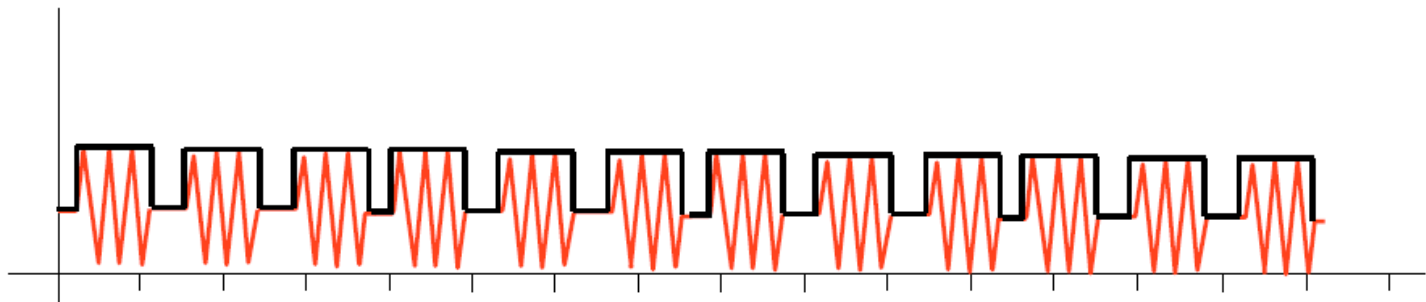
# Average power

AM



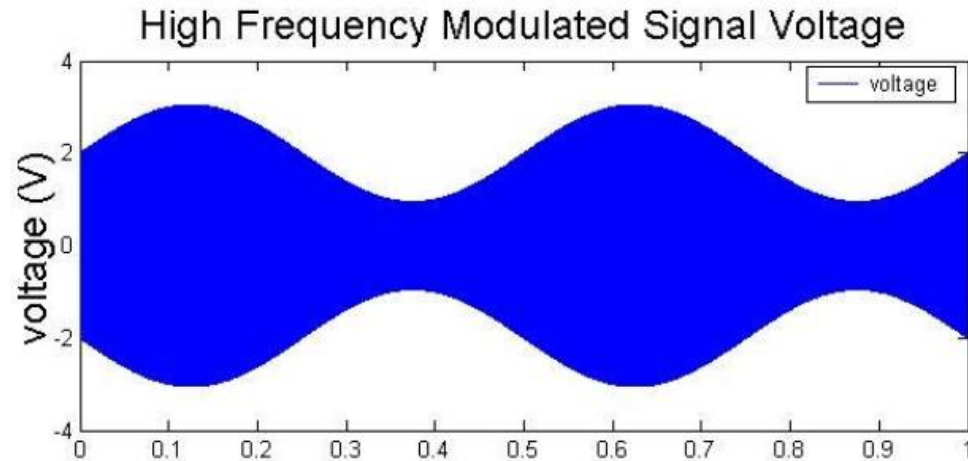
Average over many modulation cycles

Pulsed

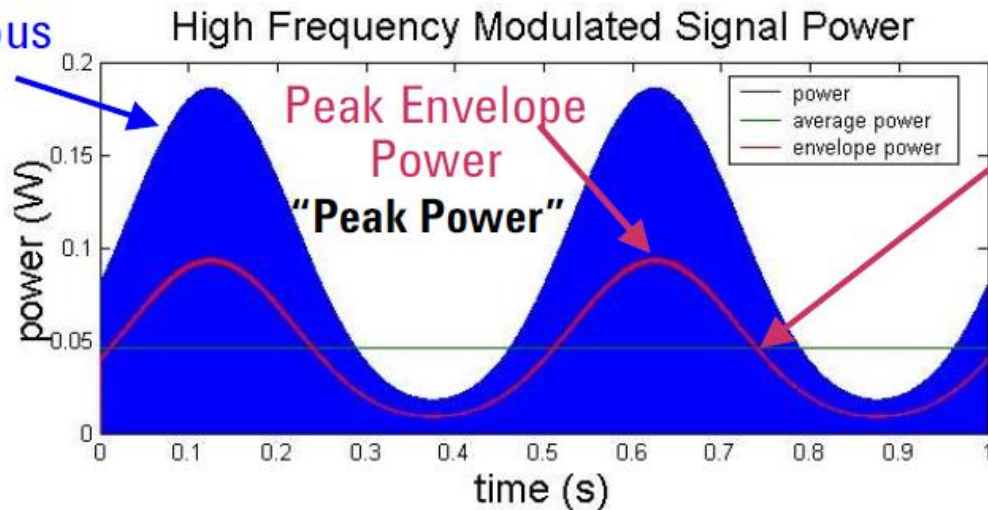


Average over many pulse repetitions

# Envelope power and Peak envelope power



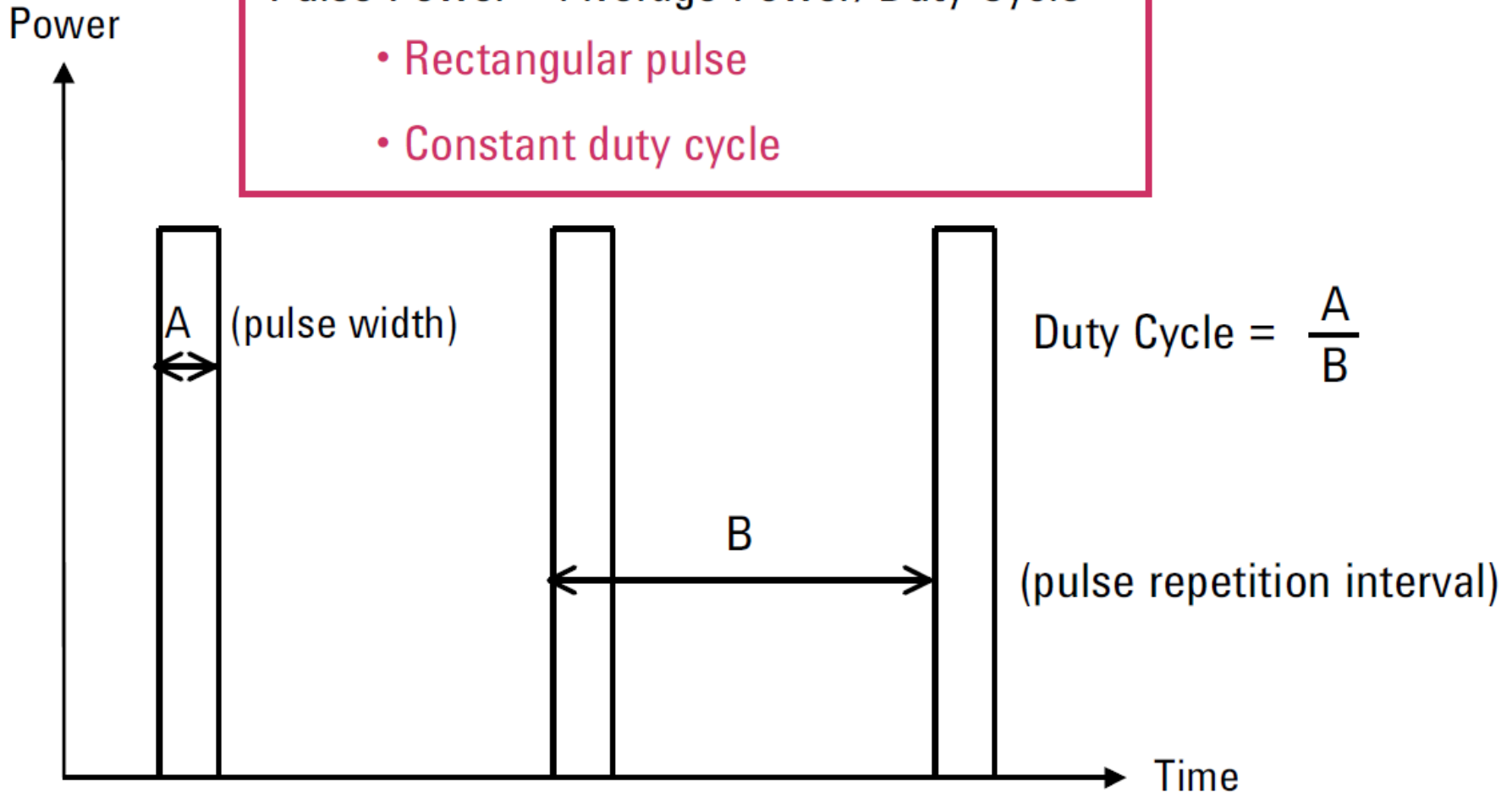
Instantaneous  
Power



# Pulse power

Pulse Power = Average Power/Duty Cycle

- Rectangular pulse
- Constant duty cycle



# Instruments

## Power Meter and Sensor



- $\pm 0.0X$  dB
- $\geq -70$  dBm

## Network Analyzer

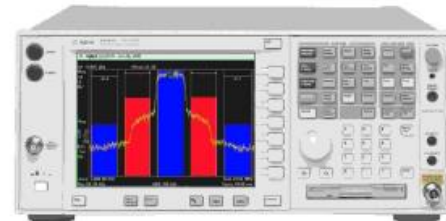


- $\pm 0. X$  dB or greater
- Frequency selective

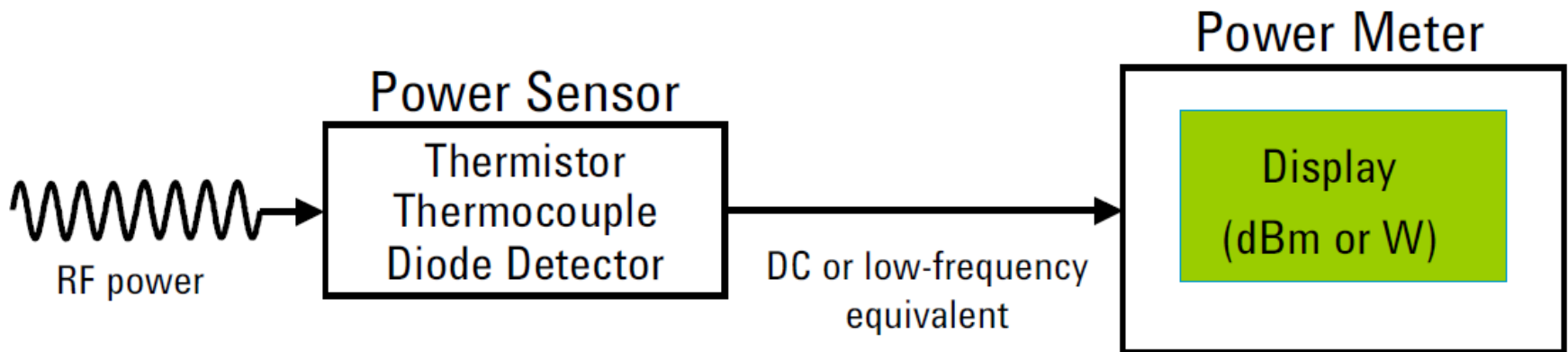
## Vector Signal Analyzer



## Spectrum Analyzer



# Power meter and sensor





# Sensor technologies

## Thermal Sensors:

power is measured by estimating the heating (in different ways)

- Calorimeters
- Bolometers (thermistors)
- Thermocouples

## Non-linear Sensors:

power is measured through a voltage measurement, after a non-linear conversion

- Diode

# Calorimeters

Calorimeters measure the heat produced by incident microwave radiation. They are typically constructed from a thermally insulating section of waveguide, a load and a temperature sensor such as a thermopile. They are in most cases the most accurate sensors available and so are used in national standards and some other calibration laboratories. Their main disadvantage is their extremely long time constant (often 20+ minutes) so they are not suitable for use in many measurement situations.

$$P = J C m \frac{dT}{dt} + \frac{T}{R}$$

$P$  = power

$C$  = specific heat

$R$  = thermal resistance.

$M$  = fluid mass

(for water  $C = 1$  kcal/kg °C;  $J = 4.18 \times 10^3$  J/kcal),



# Twin load calorimeters

Twin load calorimeters consist of two identical loads at the end of thermally insulating RF line sections within a thermally insulating container.

The temperature difference between the two loads is measured with temperature sensors. RF power can be applied to one side of the calorimeter and DC power to the other.

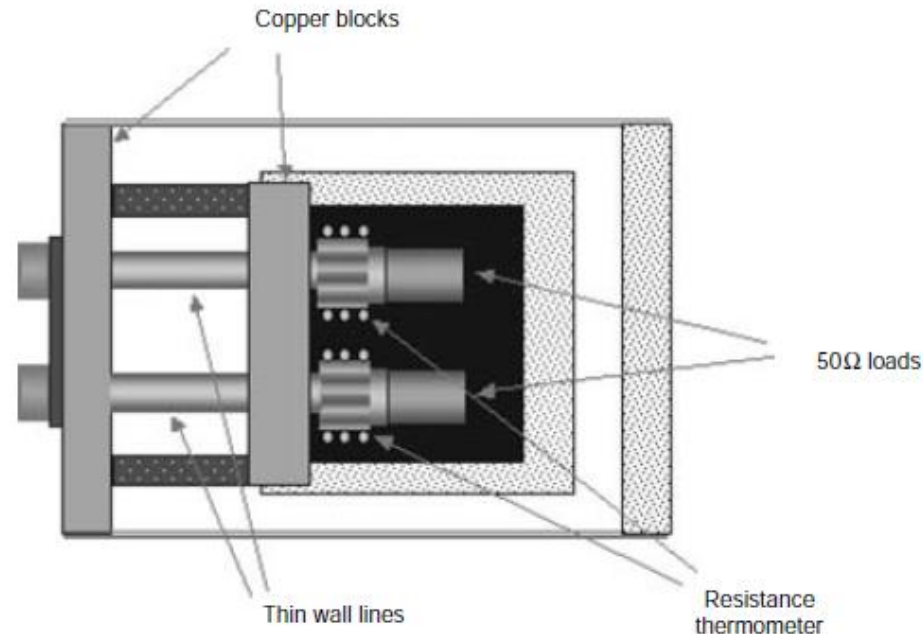
When the temperature difference between the two sides is zero the RF and DC powers can be considered equivalent.

$$P = JCm \frac{dT}{dt} + \frac{T}{R}$$

$R \rightarrow \infty$

$$P = \frac{T - T_0}{t} mCJ$$

DC or RF



# Flow calorimeters

Flow calorimeters are suitable for higher power measurements. They contain a quartz tube carrying flowing water. The power into the waveguide can be calculated by measuring the temperature rise of the water and the flow rate.

The RF power is given by:  $P=qC(T_2-T_1)J$

$T_2-T_1$  = temperature difference between input and output flow

$q$  = fluid mass flow rate

$C$  = specific heat

$J = 4.18 \times 10^3$  J/kcal

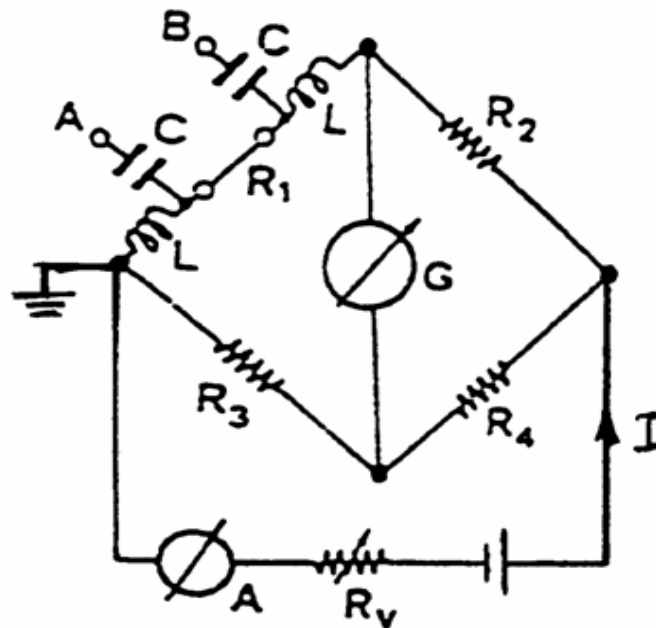
The RF heating is compared to DC heating by means of heating wires within the quartz tube that provide an identical temperature distribution.  
**(substitution technique)**

# Bolometers

The bolometers are resistors very sensitive to temperature variations.

They are generally incorporated into a Wheatstone bridge.

The RF power measurement is generally carried out by substitution, thanks to the determination of the equivalent DC power by means of the measures of  $V$  and  $R$ :



# Working principle

The bridge is balanced, therefore  $R_1=R_2$  and  $R_b=R_3$  ( $=R_0$  for RF matching)

The power dissipated by the bolometer is:

$$P_{DC} = \left( \frac{V_{A,0}}{2} \right)^2 \frac{1}{R_b} = \frac{V_{A,0}^2}{4R_0}$$

first case, without RF power

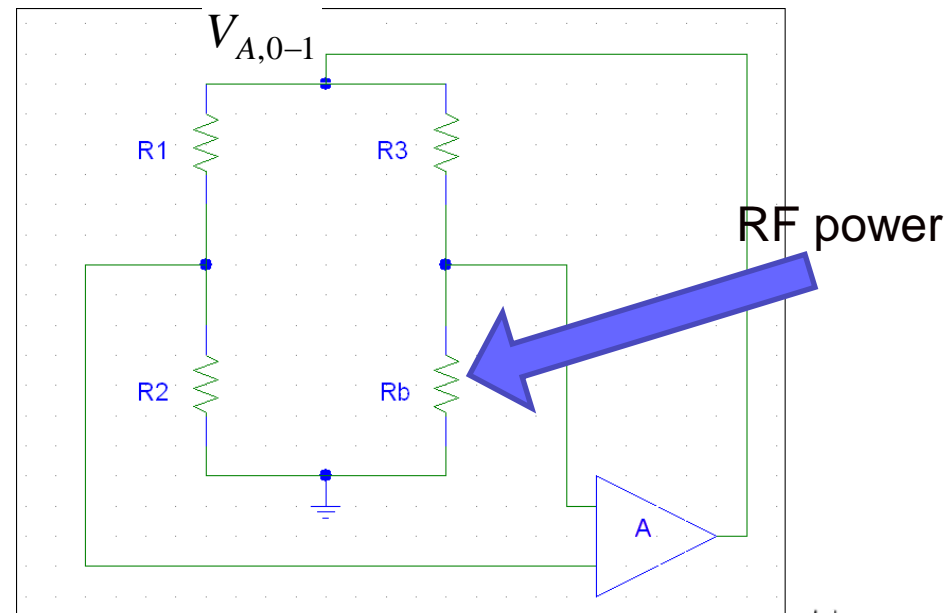
With RF power, the bolometers heats up and changes the resistance, the feedback loop acts on the DC voltage in order to keep the bridge balanced.

$$kP_{RF} + \left( \frac{V_{A,1}}{2} \right)^2 \frac{1}{R_b} = \frac{V_{A,0}^2}{4R_0}$$



$$P_{RF} = \frac{V_{A,0}^2 - V_{A,1}^2}{4kR_0}$$

$$k = \text{effective efficiency} = \frac{\text{RF power substituted by DC power}}{\text{input RF power}}$$



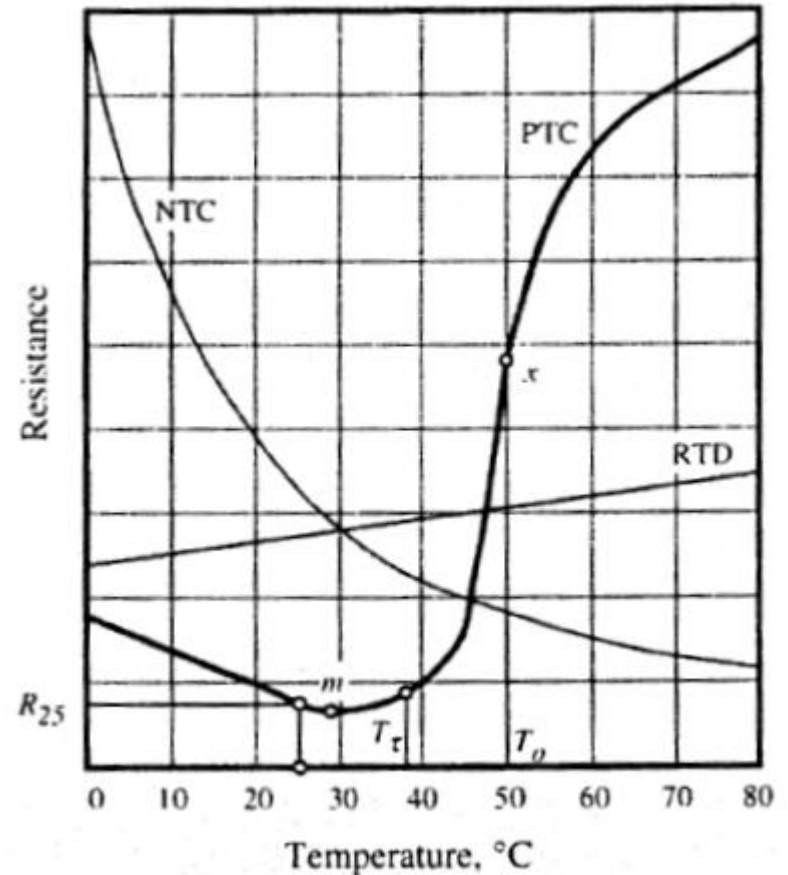
# Sensing elements

Thermistors (Negative Temperature Coefficient):

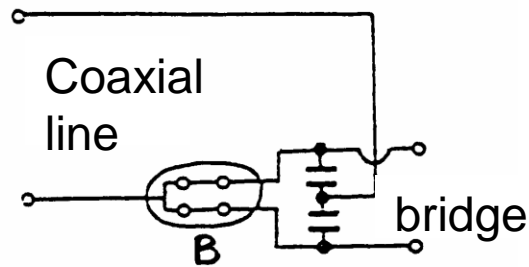
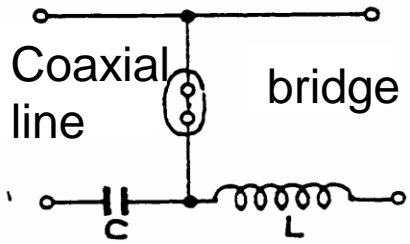
$$R = R_0 \exp \left[ -\beta \left( \frac{1}{T_0} - \frac{1}{T} \right) \right]$$

Resistance Temperature Detector  
(RTD, PT100):

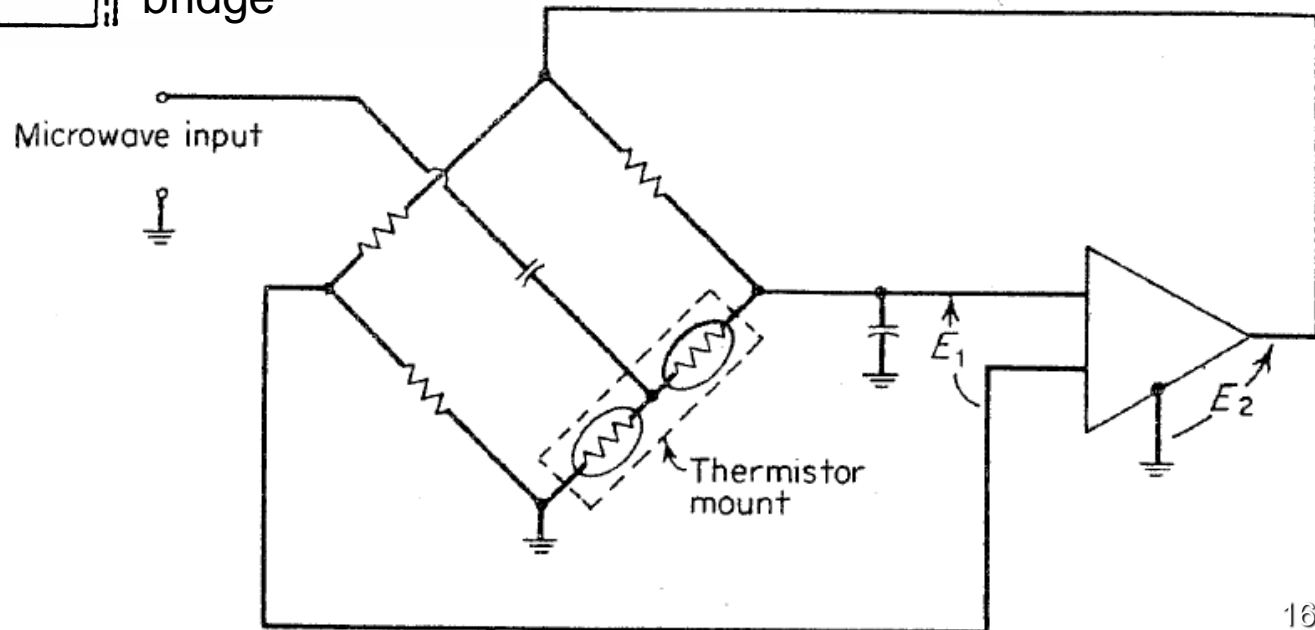
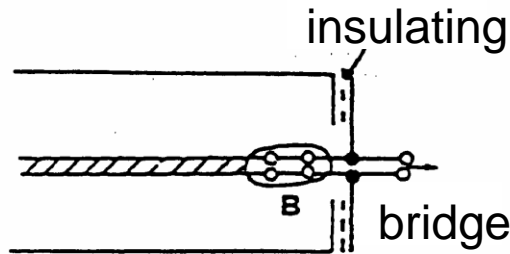
$$R = R_0 \left[ 1 + AT + BT^2 + C(T - 100)T^3 \right]$$



# Bolometers mounting



Electrical and mechanical connection to the bridge





# Measurement Errors

- Error due to the **mismatch**:

if the assembly is not adapted, a part of the power to be measured is reflected (see next slides: available power).

- **Substitution error**:

DC power and RF power do not give rise to the same thermal effects in the bolometer. The differences in behavior in the two cases are attributable both to the skin effect and the different distribution of current along the wire which constitutes the sensitive element. To reduce the error of replacement is necessary that the resistive element has a length much smaller than the wavelength and a sufficiently reduced diameter so as to obtain a current distribution as uniform as possible

- Error due to the **efficiency  $\eta$** :

$$\eta = \frac{\text{RF Power dissipated by the bolometer}}{\text{Input RF Power}}$$

It takes into account the fact that a small part of the power is dissipated on the guide walls and on the supports of the bolometer.

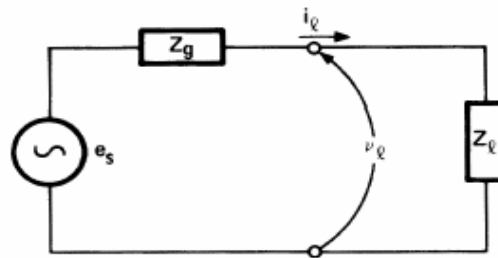
The total effect of replacing error and  $\eta$  efficiency is conglomerate in effective efficiency expression indicated by the symbol  **$K$**

# Available Power

For a low frequency circuit, formed by a generator with impedance  $Z_G$  and voltage  $e_s$  (Thevenin equivalent), the power delivered to a load  $Z_L$  is maximum when  $Z_L = Z_G^*$  (complex conjugate).

This result is achieved by maximizing the variable  $\text{Re}(v_l \times i_l)$ , as a function of  $Z_L = R_L + jX_L$ .

Such power is defined as **the available power of the generator**.

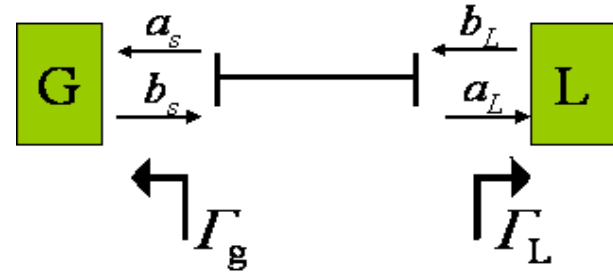


Turning to RF, with no longer voltages and currents but traveling waves  $a$  and  $b$ , the condition of maximum delivered power shifts on reflection coefficients.

# Available Power

Generator:  $b_s = \Gamma_g a_s + b_g$

Load:  $b_L = \Gamma_L a_L$



Lets consider the transmission line of negligible length:

$b_s = a_L$  and  $b_L = a_s$ .



$$a_L = \frac{b_g}{1 - \Gamma_g \Gamma_L}$$

$$b_L = \frac{b_g \Gamma_L}{1 - \Gamma_g \Gamma_L}$$

$$P = \frac{|a|^2}{2}$$



$$P_L = \frac{|a_L|^2}{2} - \frac{|b_L|^2}{2} = \frac{|b_g|^2}{2} \frac{1 - |\Gamma_L|^2}{|1 - \Gamma_g \Gamma_L|^2} = P_g \frac{1 - |\Gamma_L|^2}{|1 - \Gamma_g \Gamma_L|^2}$$

$$P_g = \frac{|b_g|^2}{2}$$

Where  $P_g$  is the power delivered to a matched load ( $\Gamma_L = 0, a_s = 0$ )

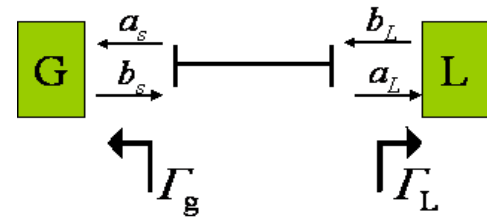
# Available Power

As for low frequency, we can demonstrate that  $P_L$  is maximum when the load reflection coefficient is equal to the complex conjugate of the reflection coefficient of the generator:

$$\Gamma_L = \Gamma_G^*$$

in this case the generator is in "**conjugate matching**", and the power transferred to the load is the maximum power-transferable = available power  $P_0$ :

$$P_0 = \frac{P_g}{1 - |\Gamma_G|^2}$$



In conclusion, the relation between the power really delivered to the load and the available power is:

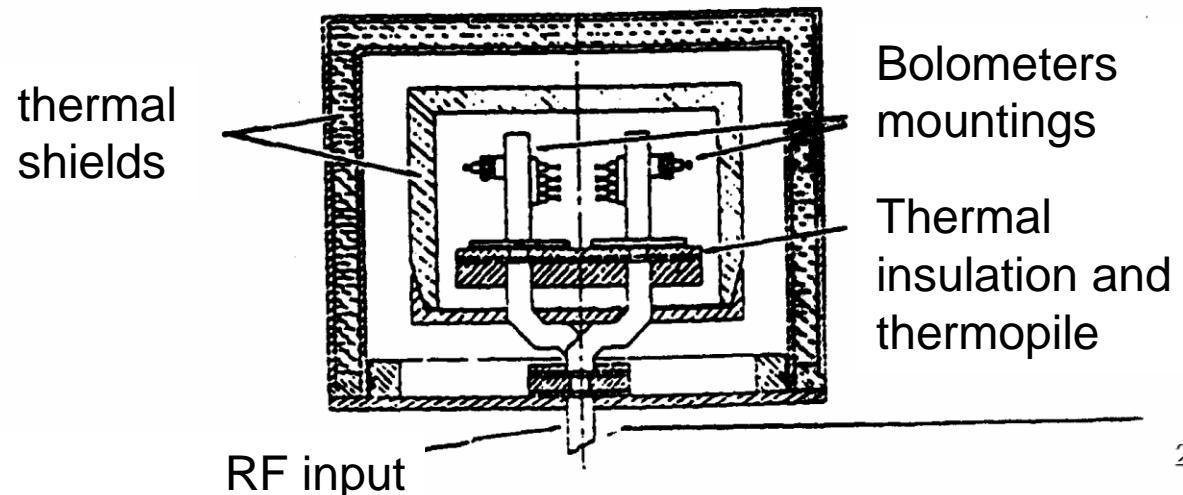
$$\frac{P_L}{P_0} = \frac{(1 - |\Gamma_g|^2)(1 - |\Gamma_L|^2)}{|1 - \Gamma_g \Gamma_L|^2}$$

# Calibration by microcalorimeter

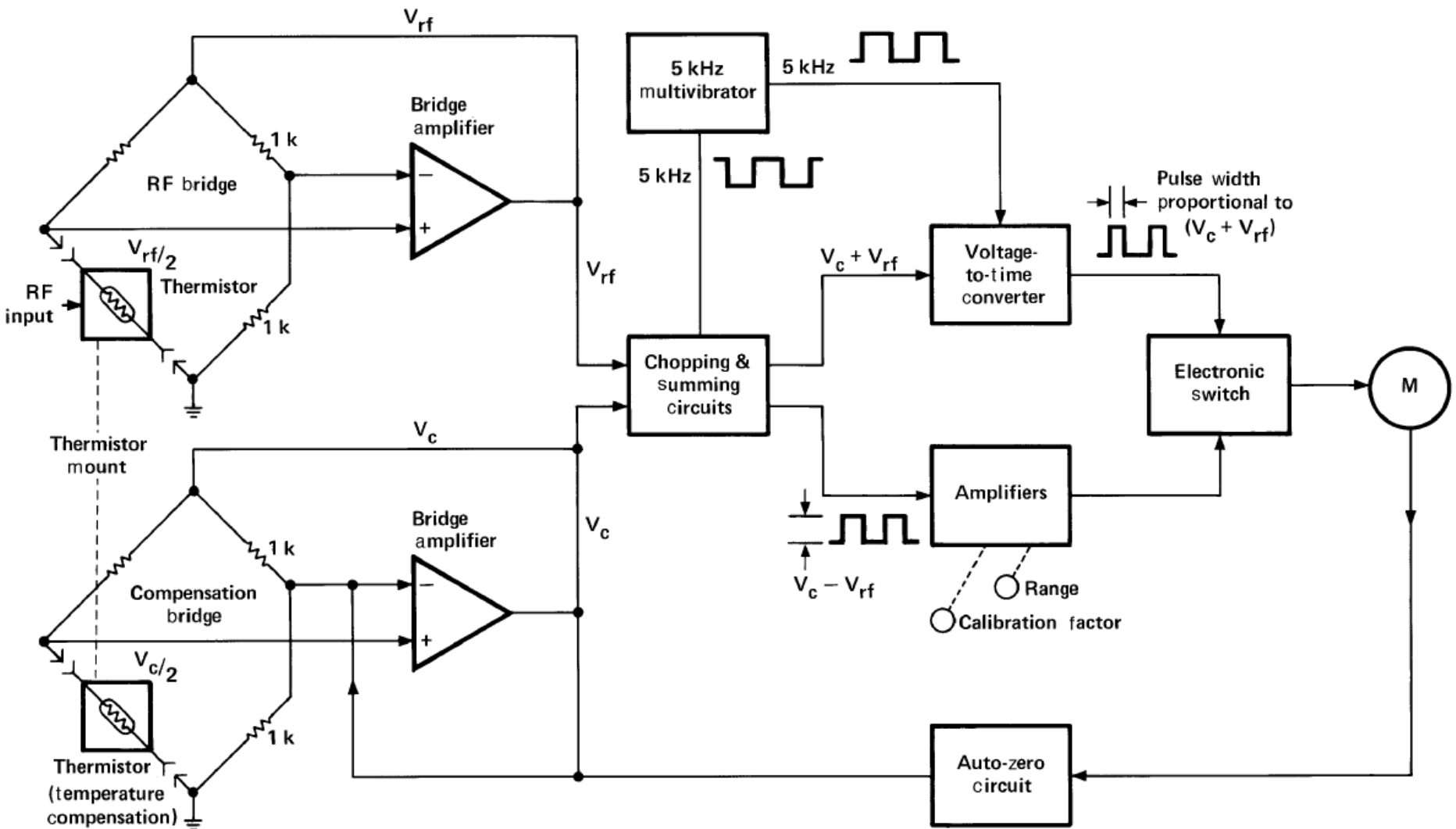
Microcalorimeters are used to calibrate thermistor type sensors.

These sensors operate in a bridge circuit such that the power dissipated in the sensor should be constant whether or not RF power is applied. The microcalorimeter measures the small temperature change caused by the extra losses in the input line of the sensor in the RF case.

A microcalorimeter consists of a thin-walled line section connected to the thermistor sensor being calibrated. A thermopile measures the temperature difference between the thermistor and a dummy sensor or temperature reference. By measuring the temperature change due to the RF loss in the sensor and the input line, the efficiency of the sensor can be calculated.



# Balanced system



# Thermocouple

Thermocouples are based on the fact that dissimilar metals generate a voltage due to temperature differences at a hot and a cold junction of the two metals.

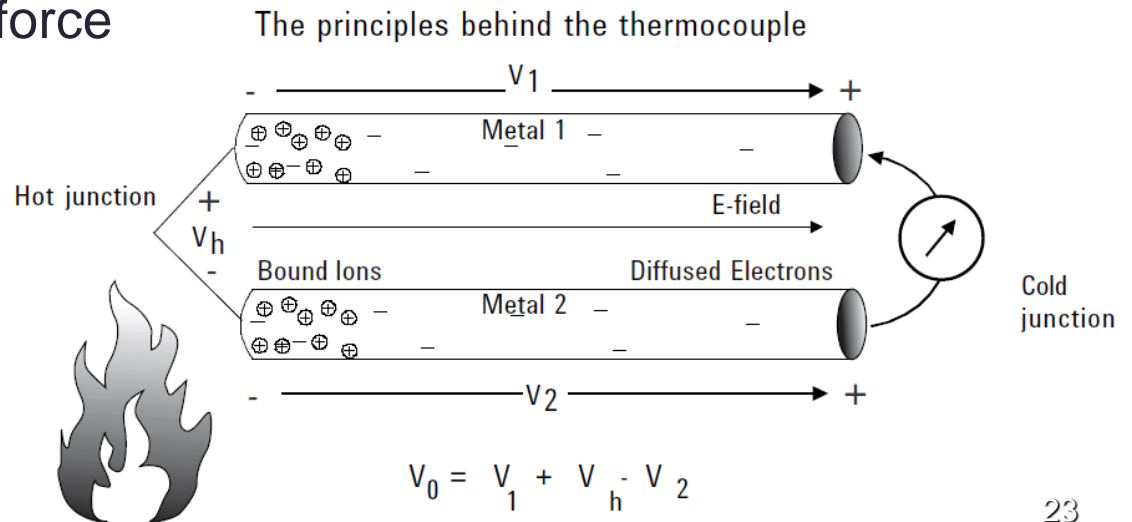
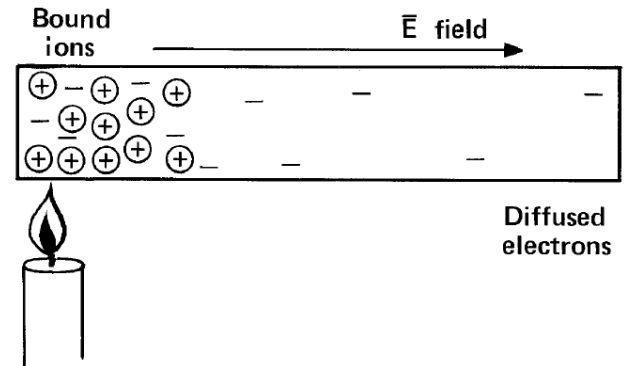
Thomson electromotive force

+

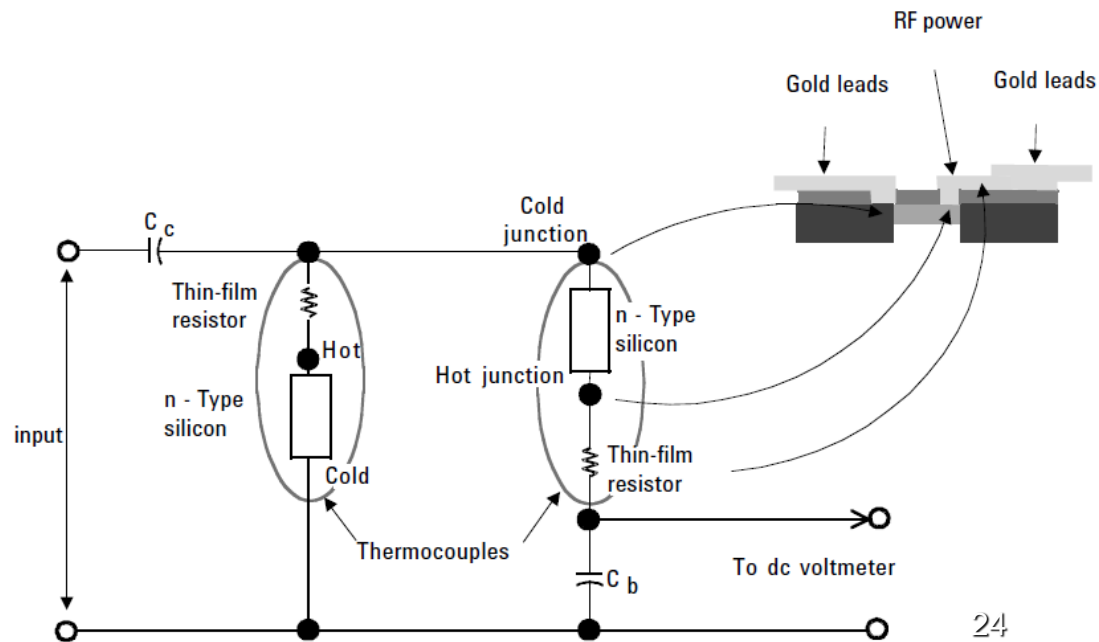
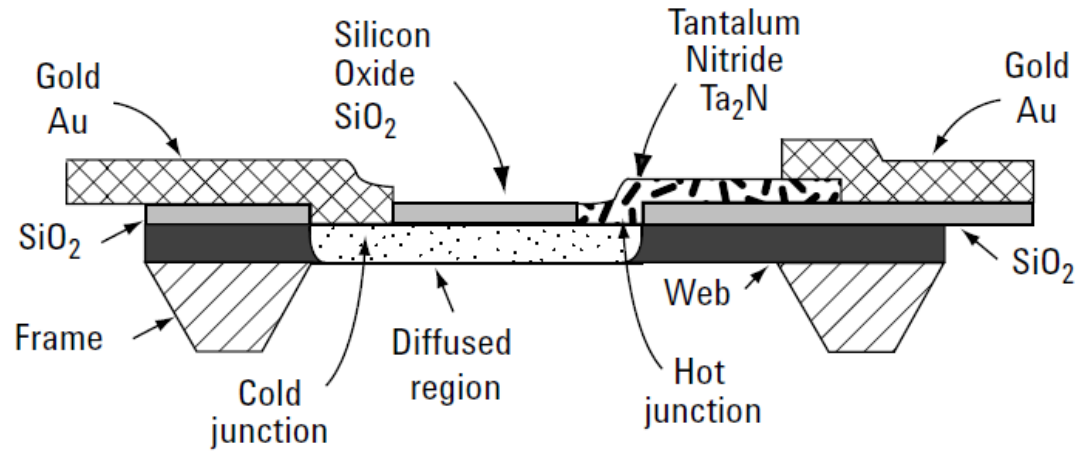
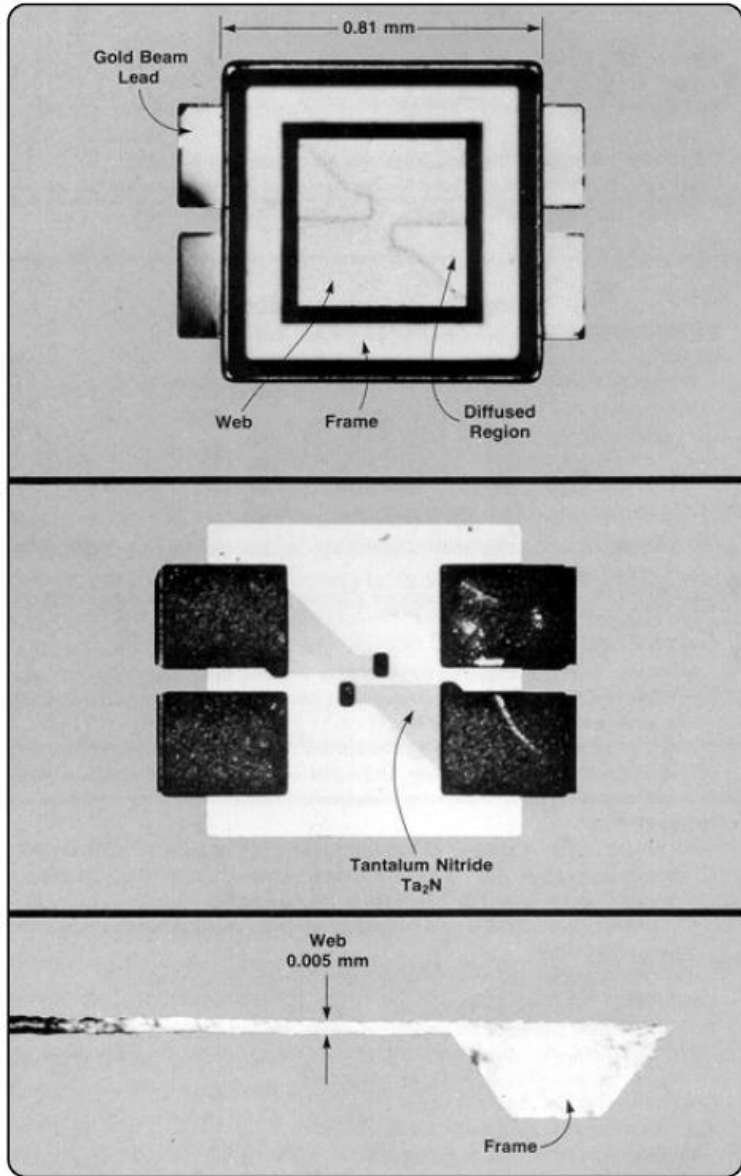
Peltier effect

=

Seebeck electromotive force



# Thermocouple Sensor





# Sensitivity

Thermoelectric power **250  $\mu\text{V}/^\circ\text{C}$**  (Si-Ta<sub>2</sub>N)

The thermocouple has a thermal resistance **0.4  $^\circ\text{C}/\text{mW}$** .

Thus, the overall sensitivity of each thermocouple is 100  $\mu\text{V}/\text{mW}$ .

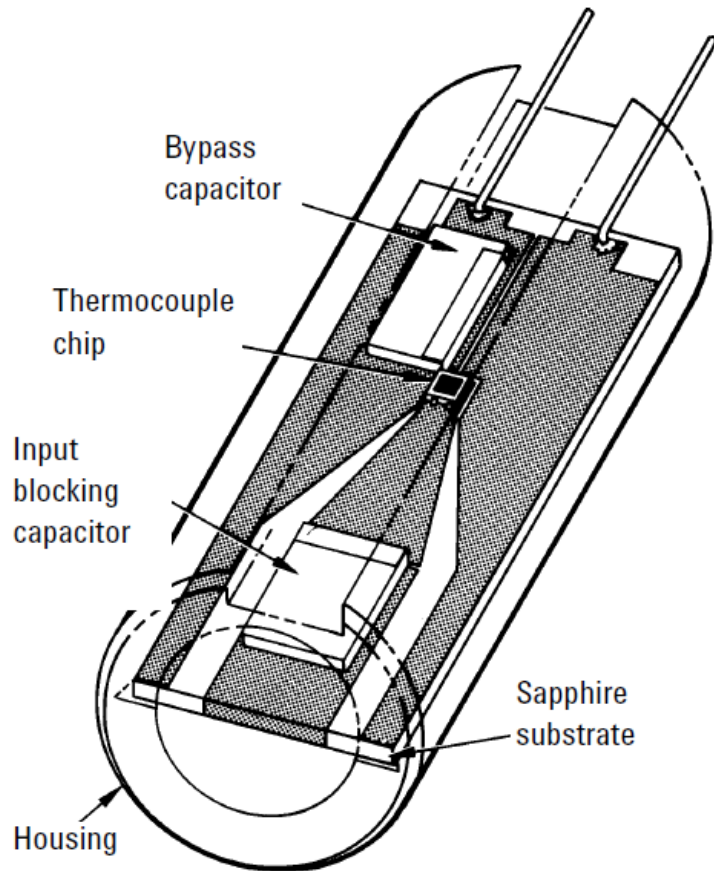
Two thermocouples in series yield a sensitivity of **160  $\mu\text{V}/\text{mW}$**  because of thermal coupling between the thermocouples.

If the hot junction rises to 500  $^\circ\text{C}$ , differential thermal expansion causes the chip to fracture.

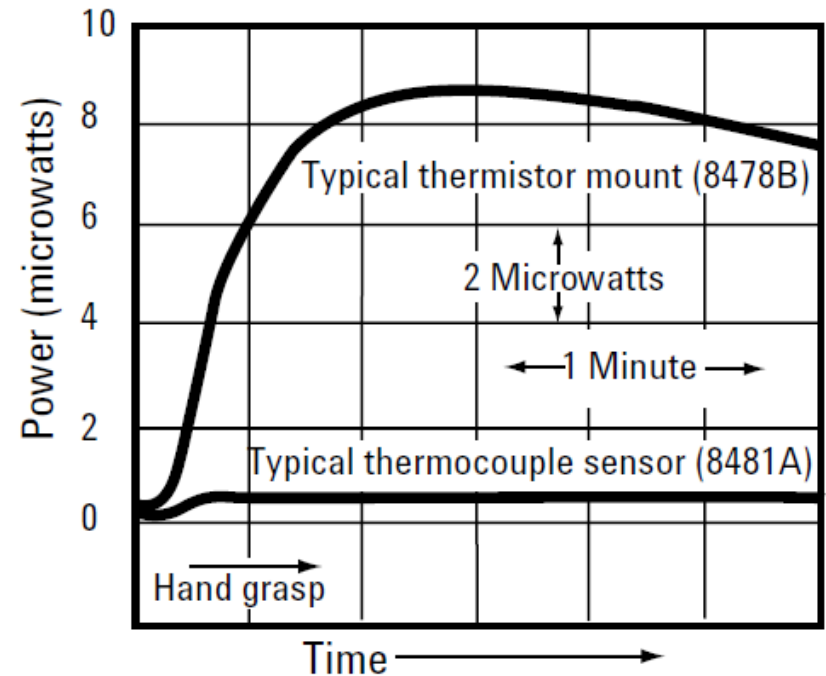
Thus, the sensor is limited to **300 mW maximum average power**.

The thermal resistance combines with the thermal capacity to form the thermal time constant of **120  $\mu\text{s}$** .

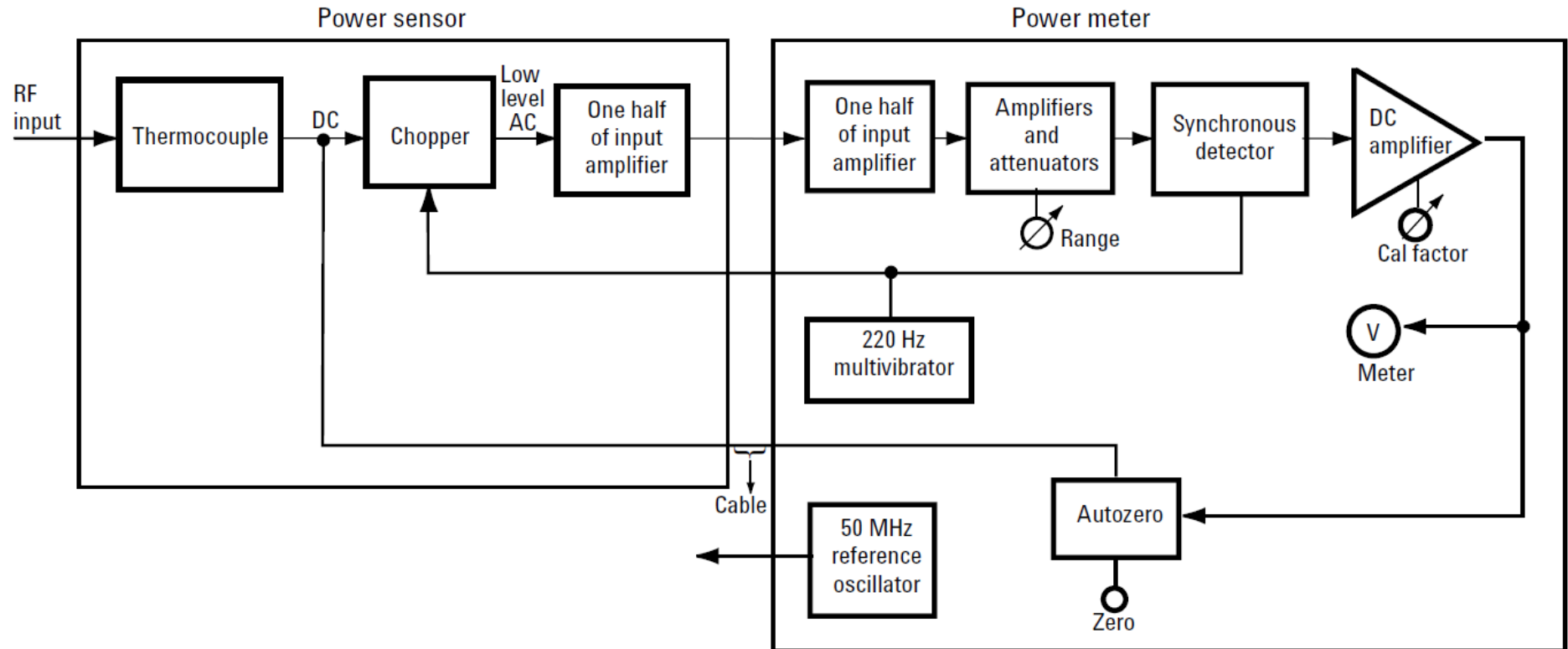
# Layout – sensitivity to temperature



**Zero drift of thermocouple and thermistor power sensors due to being grasped by a hand.**



# Power meter for thermocouple sensors



Accuracy: (for 2 years)

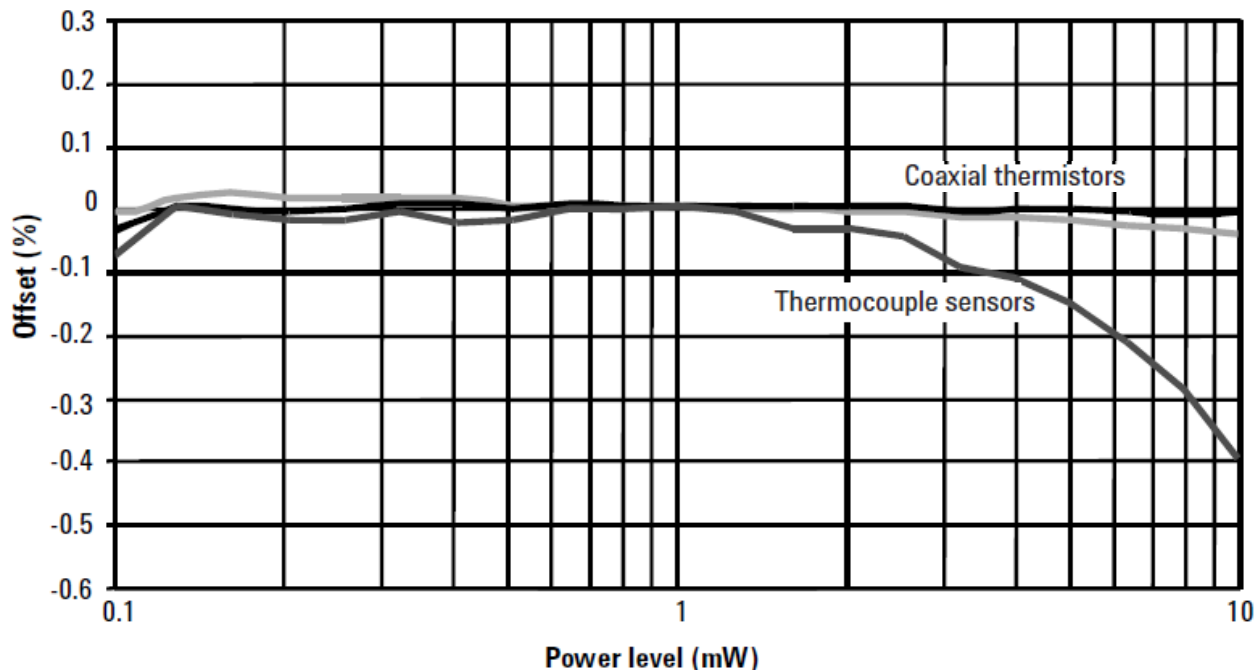
$\pm 0.5\%$  ( $23 \pm 3$  °C)

$\pm 0.6\%$  ( $25 \pm 10$  °C)

$\pm 0.9\%$  (0 - 55 °C)

# Calibration and linearity

In the case of thermistor sensors, the DC-substitution process keeps the tiny bead of thermistor, at a constant temperature, backing off bias power as RF power is added. In the case of thermocouple sensors, as power is added, the detection microcircuit substrate with its terminating resistor runs at higher temperatures as the RF power increases. This naturally induces minor deviations in the detection characteristic.



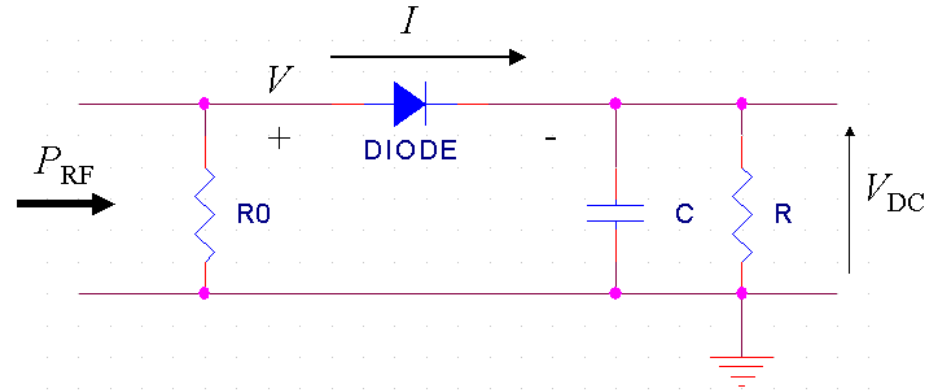
Thermocouple power meters solve the need for sensitivity calibration by **incorporating a 50 MHz power-reference oscillator** whose output power is controlled with great precision ( $\pm 0.4\%$ ).

# Diode sensor

We can consider the simplified circuit shown in figure, with an input matching impedance  $R_0 = 50 \Omega$

$$I = I_s [\exp(V/nV_T) - 1],$$

$$V_T = kT/e \cong 25 \text{ mV}$$

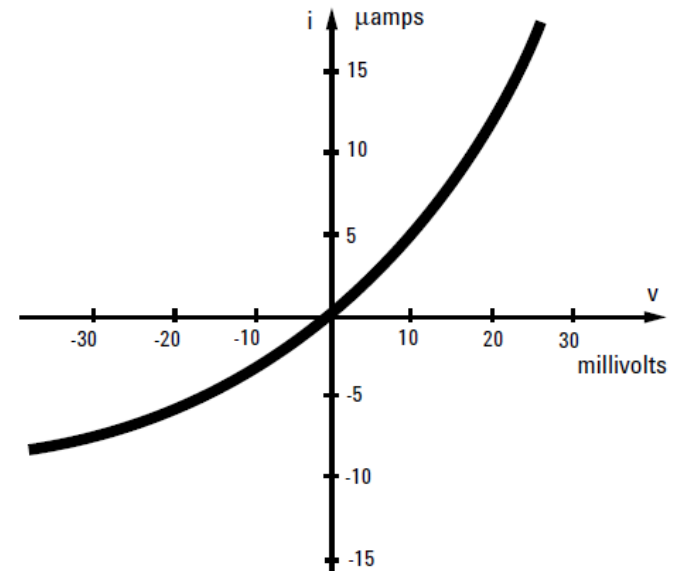


In order to describe the diode behavior for low voltages, we can develop in series the exponential

$$I = I_s \left( \frac{V}{nV_T} + \frac{V^2}{2(nV_T)^2} + \frac{V^3}{3!(nV_T)^3} + \dots \right)$$

If we consider an input sinusoidal voltage  $V$ , due to the input power  $R_0$ , with  $V = V_{RF} \sin(\omega t)$  and thus

$$P_{RF} = \frac{V_{RF}^2}{2R_0}$$



# Diode sensor

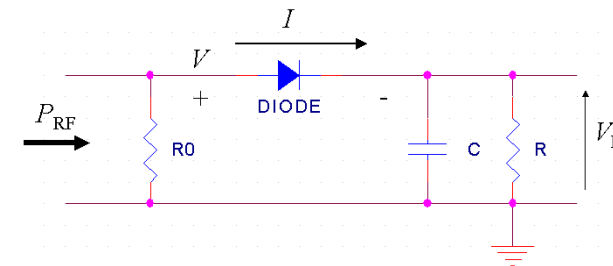
For very-low voltages  $V \ll V_T$  we can stop the series to the second term, neglecting the contribution of the higher-order terms.

In this approximation, the DC component of the current, equal to the average value of  $I$  is given by:

$$I_{DC} = \langle I \rangle = I_s \frac{\langle V^2 \rangle}{2(nV_T)^2} = I_s \frac{V_{RF}^2 \langle \sin^2(\omega t) \rangle}{2(nV_T)^2} = I_s \frac{V_{RF}^2}{4(nV_T)^2}$$

The differential resistance  $R_D$  of the diode is given by:

$$\frac{1}{R_D} = \left. \frac{\partial I}{\partial V} \right|_{I=0} = \frac{I_s}{nV_T}$$



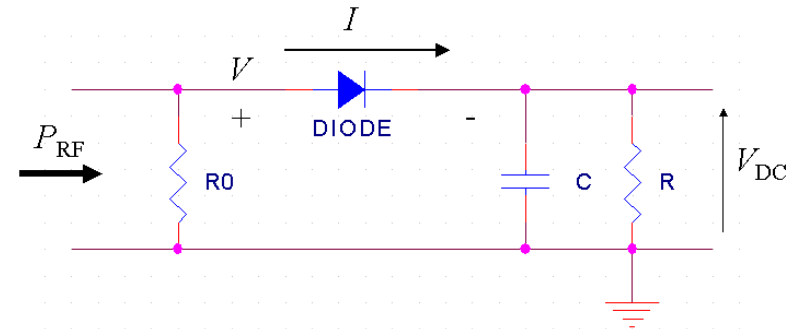
For a RF diode, the saturation current has value close to 10  $\mu\text{A}$ , hence its differential resistance is equal to some  $\text{k}\Omega$ : being  $R_D \gg R_0$ , the diode presence does not compromise the input line matching.

The current  $I_{DC}$  falls on the diode differential resistance  $R_D$  in parallel with the load  $R$ , whose value is  $\gg R_D$ . In this way we obtain an output DC voltage equal to:

$$V_{DC} = I_{DC} R_D = R_D I_s \frac{V_{RF}^2}{4(nV_T)^2} = \frac{V_{RF}^2}{4nV_T} = \frac{R_0}{2nV_T} P_{RF}$$

# Diode sensor

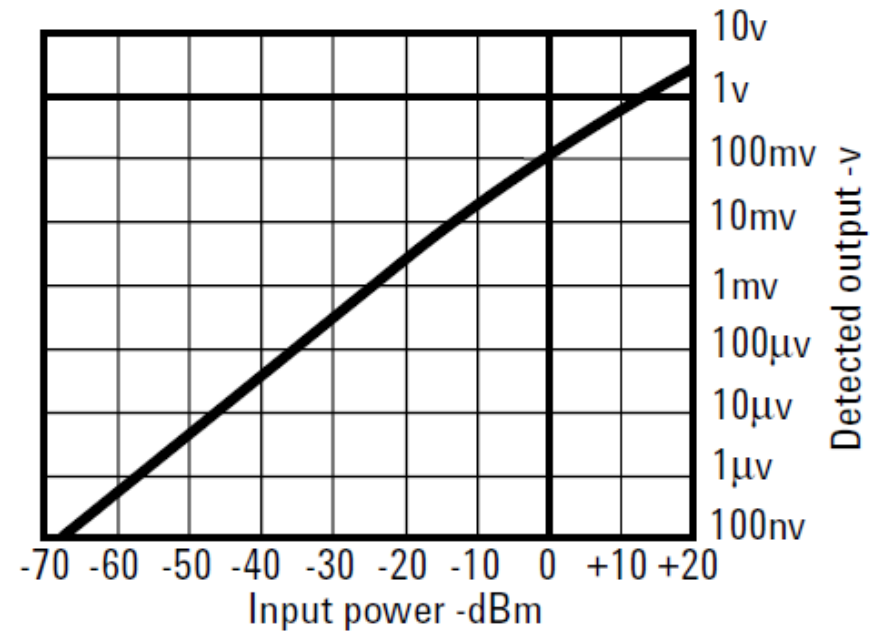
$$V_{DC} = \frac{R_0}{2nV_T} P_{RF}$$



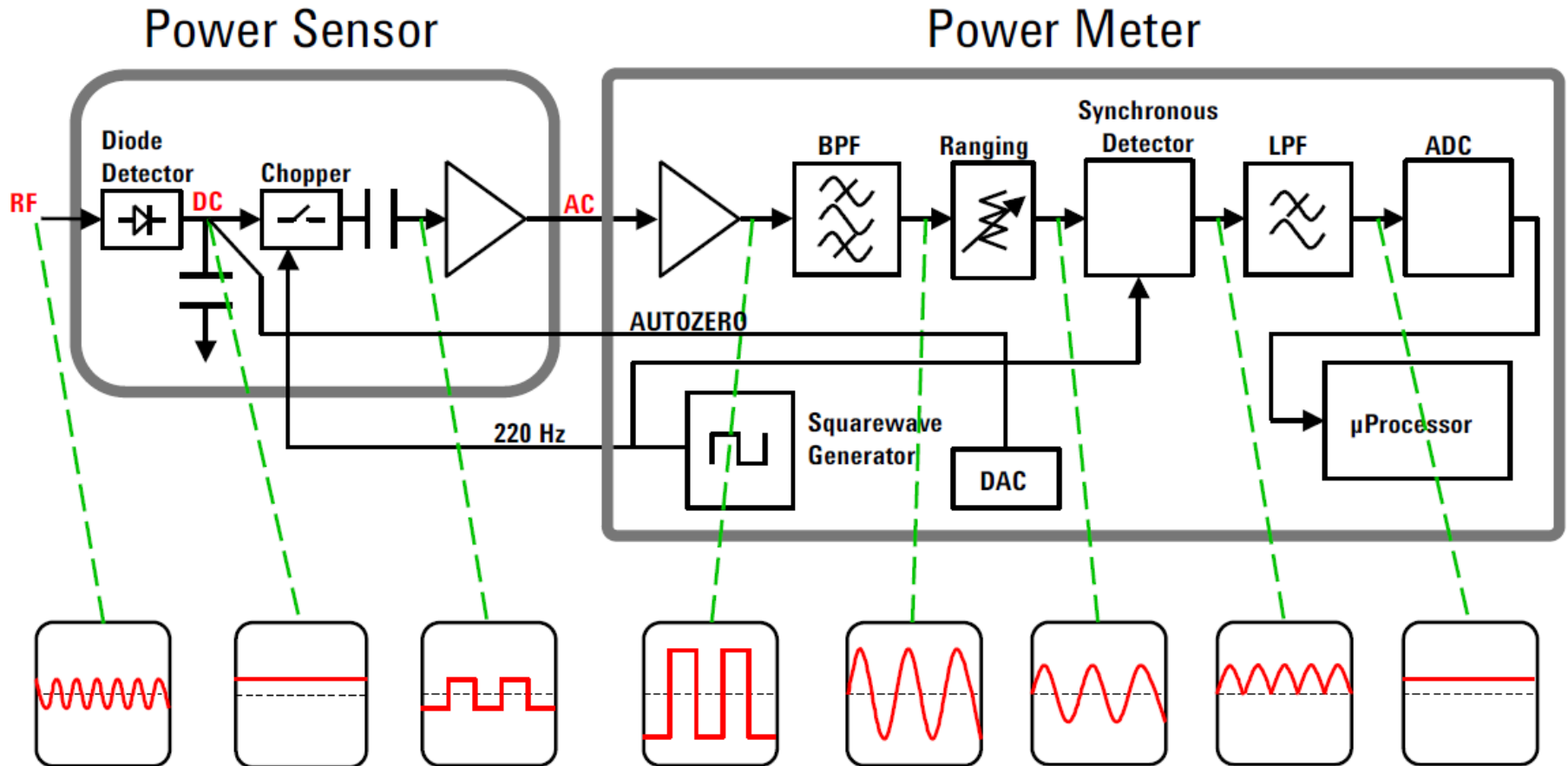
We get a sensitivity between **0.5 mV/ $\mu$ W** and **1 mV/ $\mu$ W**.

Considering a noise floor equal to 100 nV, for example, the minimum RF input power is about **-70 dBm**, which is the noise background of this type of detectors.

This discussion does not consider the non-ideality of the circuit and of the diode itself, and is mathematically valid only for input powers below -20 dBm, power level corresponding to the condition  $V < V_T$ .



# Power sensor and Meter signal path

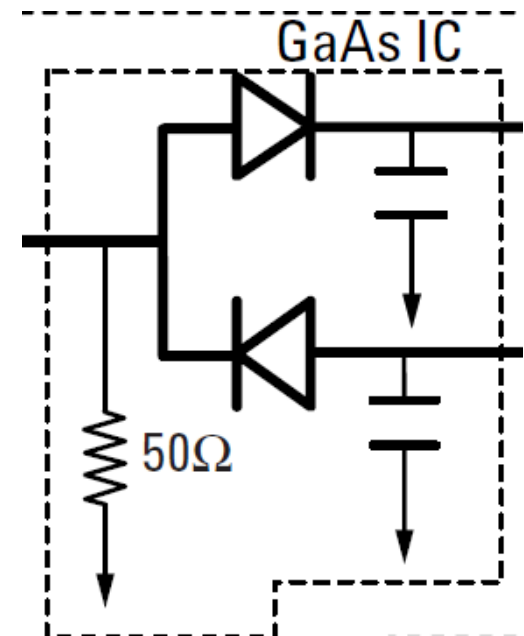




# Differential scheme

## Advantages:

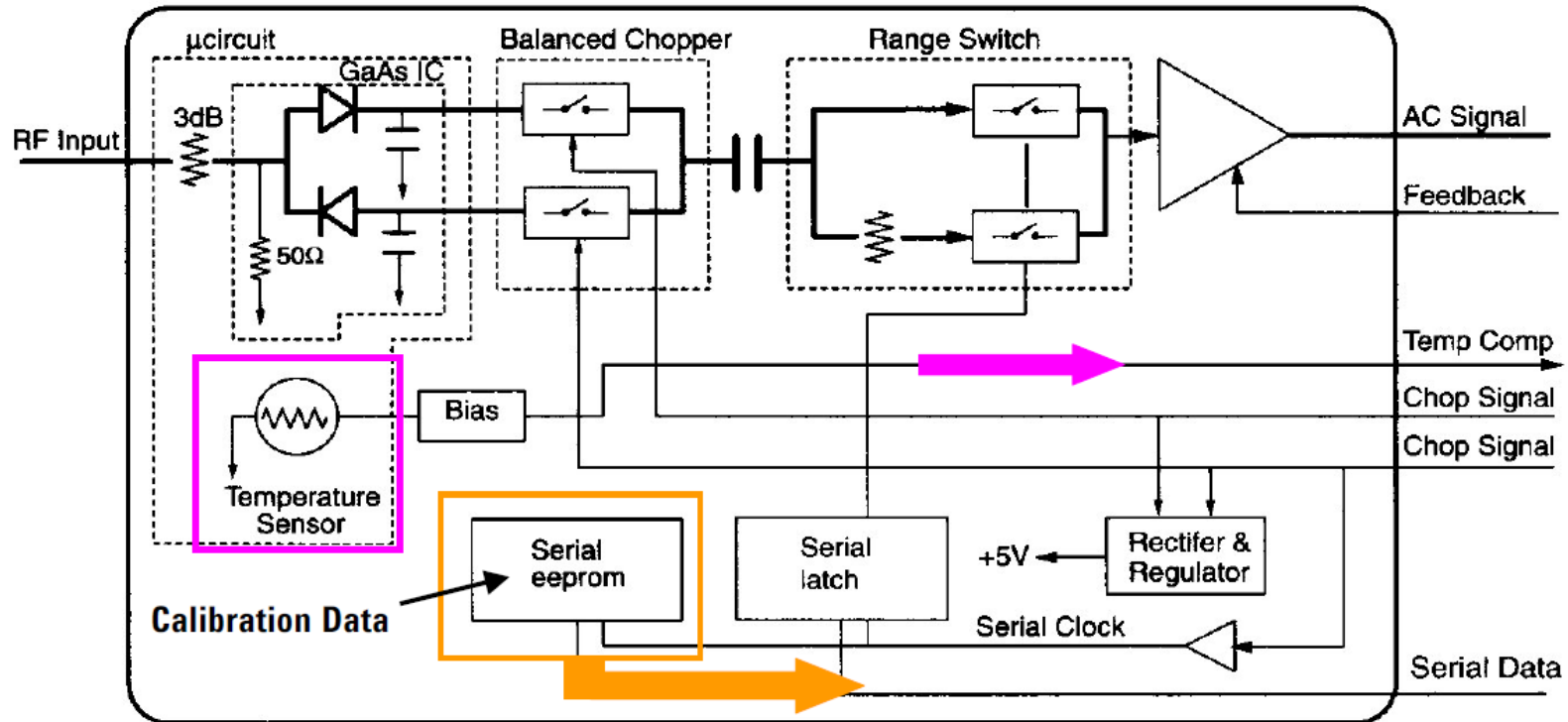
- Thermoelectric voltages resulting from the joining of dissimilar metals, a serious problem below  $-60$  dBm, are cancelled.
- Measurement errors caused by even-order harmonics in the input signal are suppressed due to the balanced configuration.
- A signal-to-noise improvement of 1 to 2 dB is realized by having two diodes.
- The detected output signal is doubled in voltage (quadrupled in power) while the noise output is doubled in power since the dominant noise sources are uncorrelated.
- Common-mode noise or interference riding on the ground plane is cancelled at the detector output. This is not RF noise but metallic connection noises on the meter side.



Diode technology provides some 3000 times (35 dB) more efficient RF-to-DC conversion compared to the thermocouple sensors

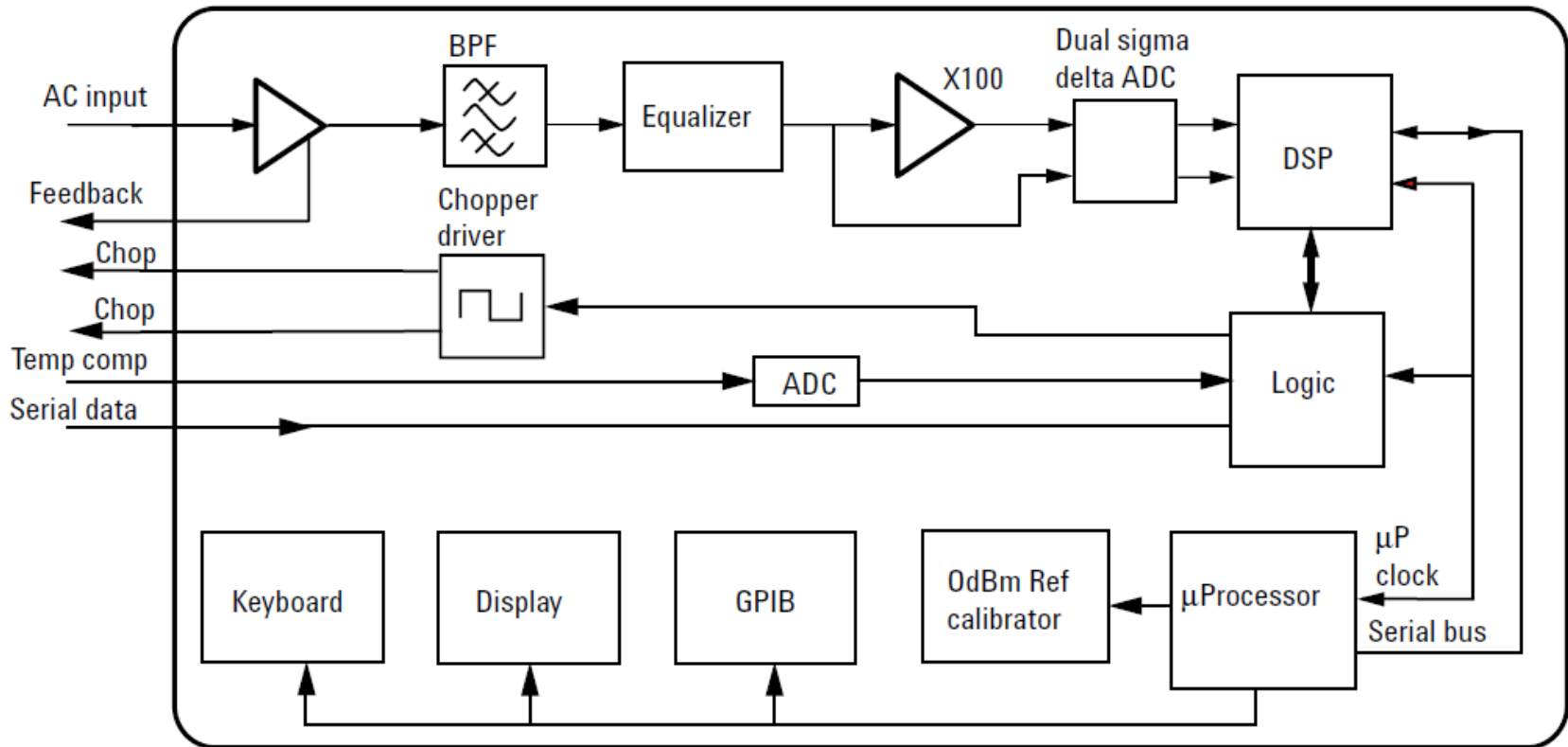
# CW Power Sensor

- 70 to + 20 dBm = 90 dB Dynamic Range



To achieve the expanded dynamic range of 90 dB, the sensor/meter architecture depends on a data compensation algorithm that is calibrated and stored in an individual EEPROM in each sensor. The data algorithm stores information of three parameters, input power level vs frequency vs temperature for the range 10 MHz to 18 or 26.5 GHz and -70 to +20 dBm and 0 to 55 °C.

# CW Power Sensor

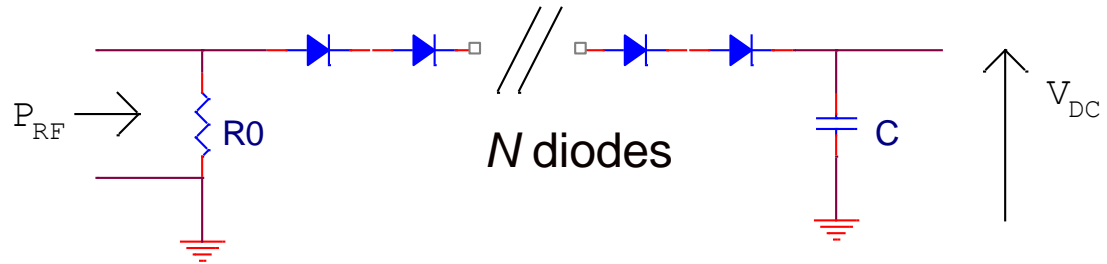


The power meter uses the uploaded calibration data from each connected sensor to compensate for the three critical sensor parameters, power from  $-70$  to  $+20$  dBm, frequency for its specified band, and operating temperature

# Diodes in series

The RF voltage on each diode is divided by  $N$ :

$$V_{1D} = \frac{V_{RF}}{N}$$



The generated DC current is the same for each diode:

$$I_{DC} = I_s \frac{V_{1D}^2}{4(nV_T)^2} = I_s \frac{V_{RF}^2}{N^2 4(nV_T)^2} = \frac{I_{DC,1diode}}{N^2}$$

The resistance of the series is:

$$R_{D,N \text{ diodes}} = N \cdot R_D$$

The voltage DC is:

$$V_{DC} = I_{DC} R_{D,N \text{ diodes}} = \frac{I_{DC,1diode}}{N^2} N \cdot R_D = \frac{V_{DC,1diode}}{N} = \frac{R_0}{2nV_T} \frac{P_{RF}}{N}$$

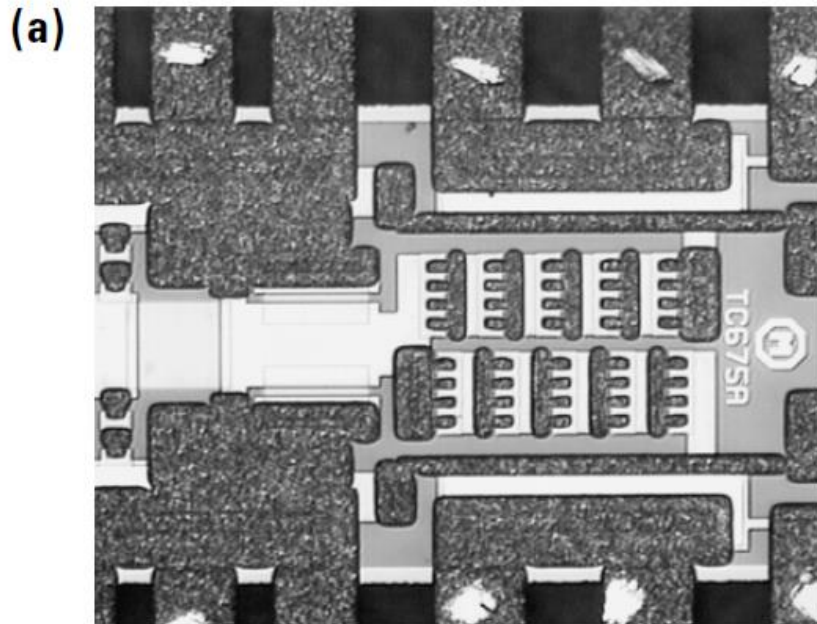


The sensitivity is divided by  $N$  → the noise power level grows of  $10\log_{10}(N)$  but the maximum power for the quadratic region is increased by  $N^2$  [ $20\log_{10}(N)$ ]

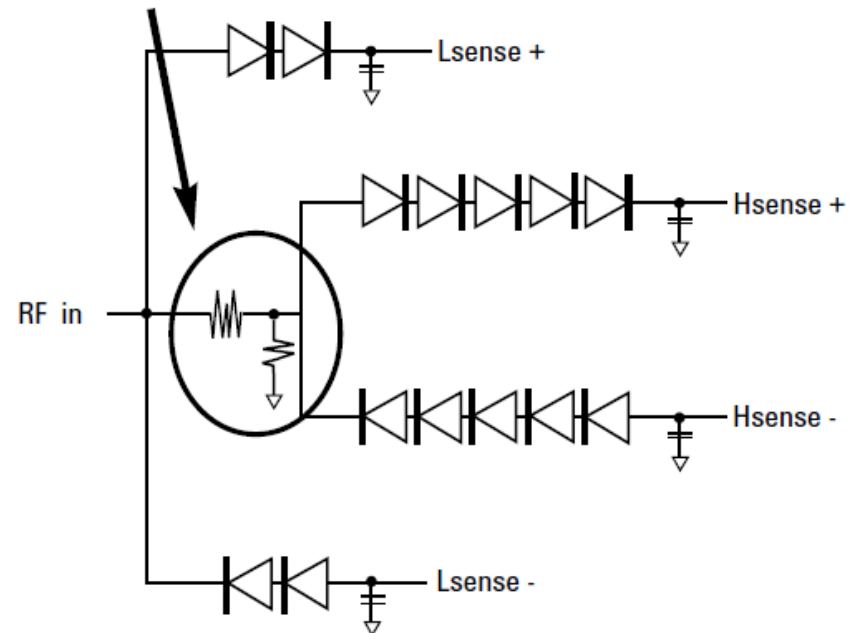
**The dynamic range is improved by  $10\log_{10}(N)$**

# Wide-dynamic-range power sensors

The Agilent E-Series E9300 power sensors are implemented as a modified barrier integrated diode (MBID) with a two diode stack pair for the low power path ( $-60$  to  $-10$  dBm), a resistive divider attenuator and a five diode stack pair for the high power path ( $-10$  to  $+20$  dBm),



(b) Resistive power splitter

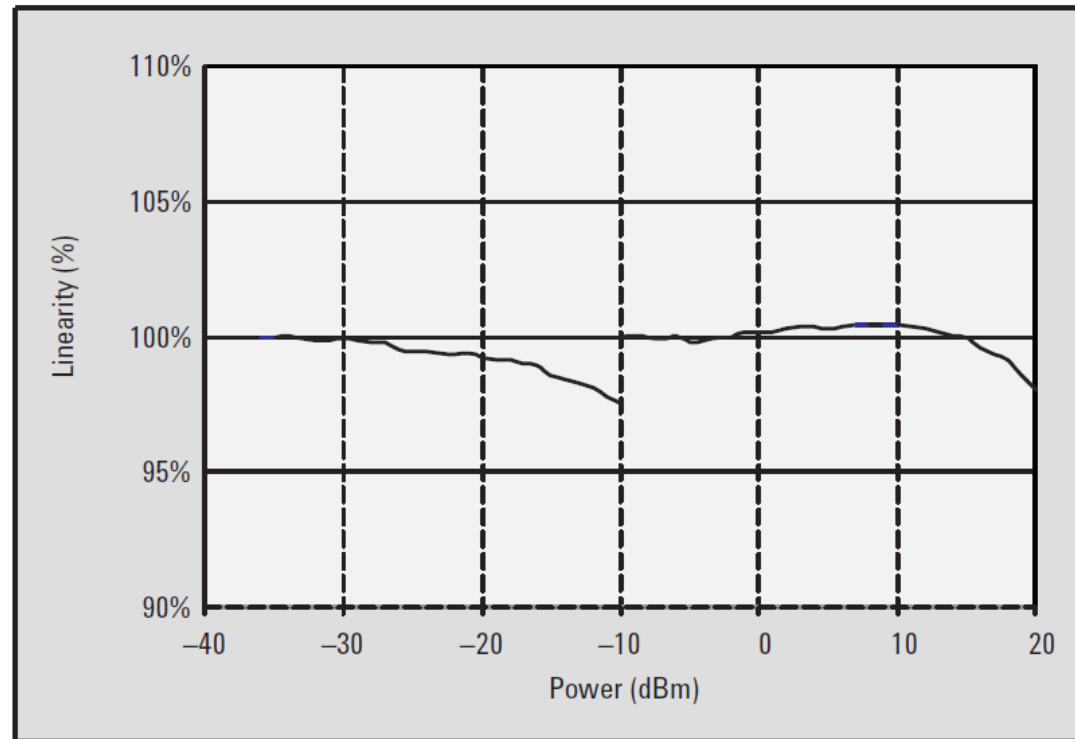


# Linearity and calibration

All thermocouple and diode power sensors require a power reference to absolute power, traceable to the manufacturer or national standards. Power meters accomplish this power traceability by use of a highly stable, internal 50 MHz power reference oscillator.

The 1 mW reference power output is near the center of the dynamic range of thermocouple power sensors, but above the range of the sensitive diode sensor series. Therefore, a special 30 dB calibration attenuator, designed for excellent precision at 50 MHz (1%), is supplied with each diode power sensor.

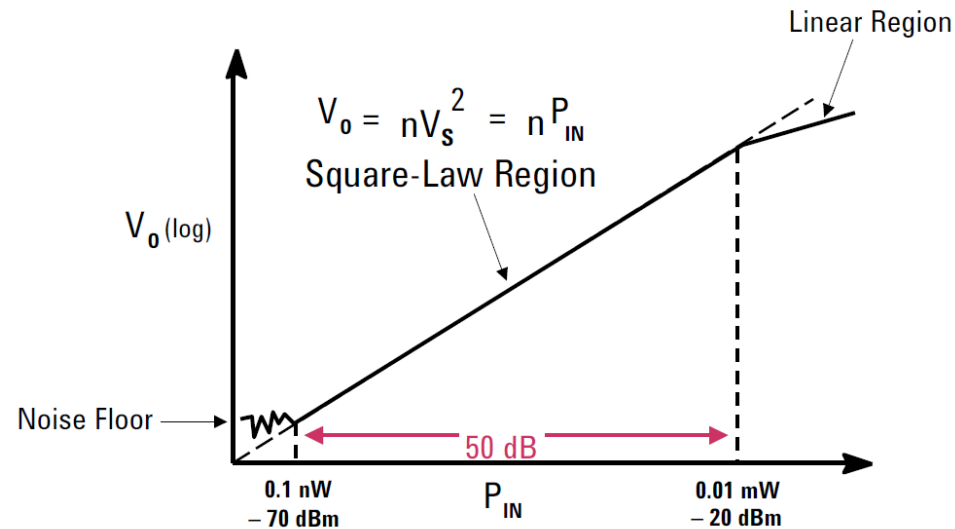
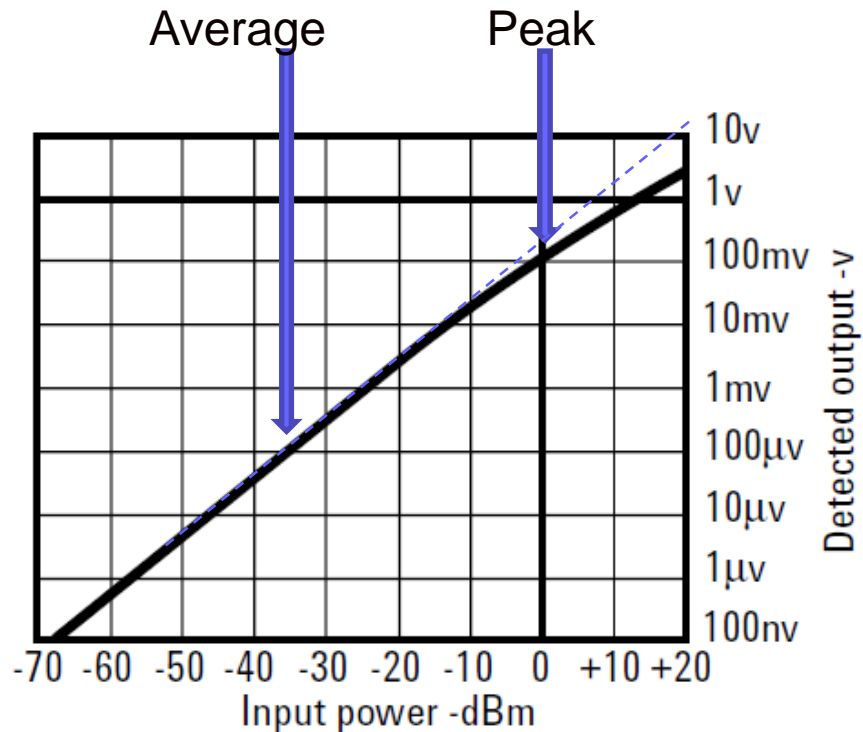
Power range	Linearity (25 ±10 °C)	Linearity (0 to 55 °C)
-60 to -10 dBm	± 3.0%	± 3.5%
-10 to 0 dBm	± 2.5%	± 3.0%
0 to +20 dBm	± 2.0%	± 2.5%



# Problems with non-CW signals

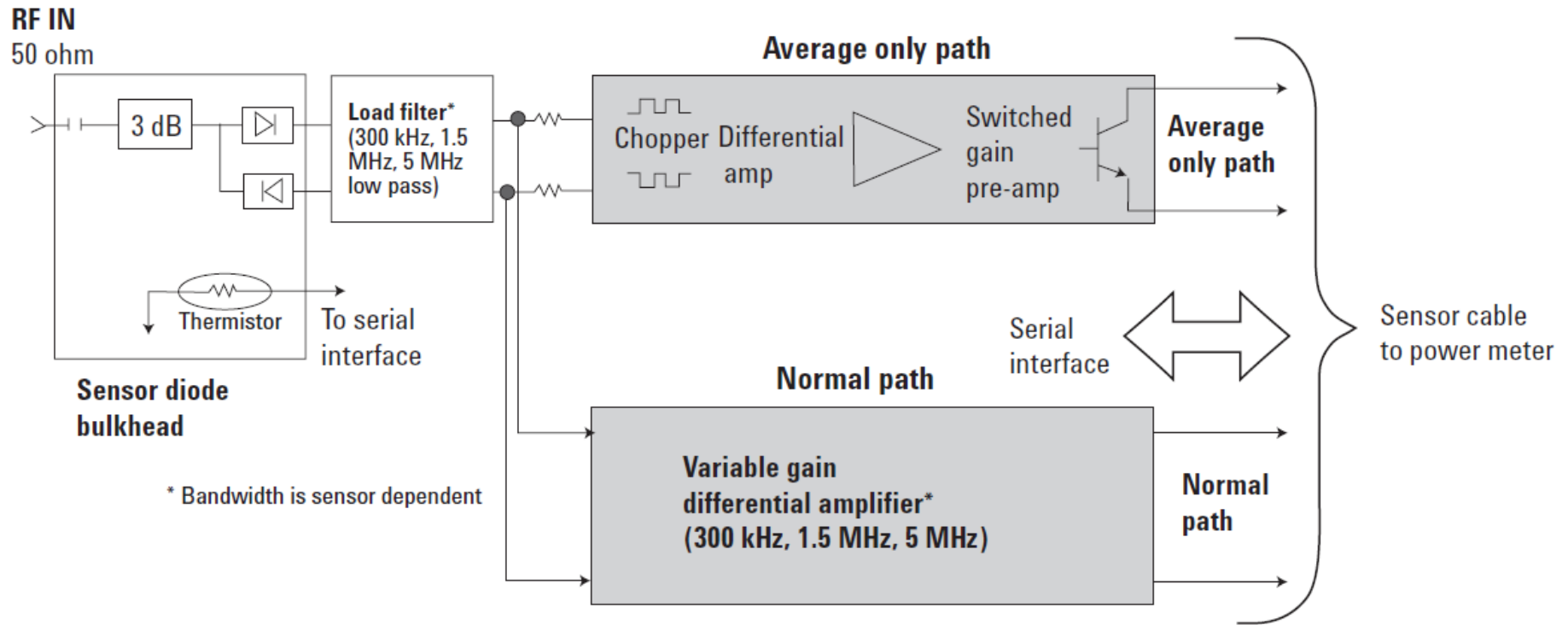
If the instantaneous power is much higher than the average power, the non linearity in the diode characteristic can induce measurement error.

Problem with high crest factor signals (crest factor = peak value / rms value)



For non-CW signals with average powers between -20 and +20 dBm, use the thermocouple sensors for true average power sensing.

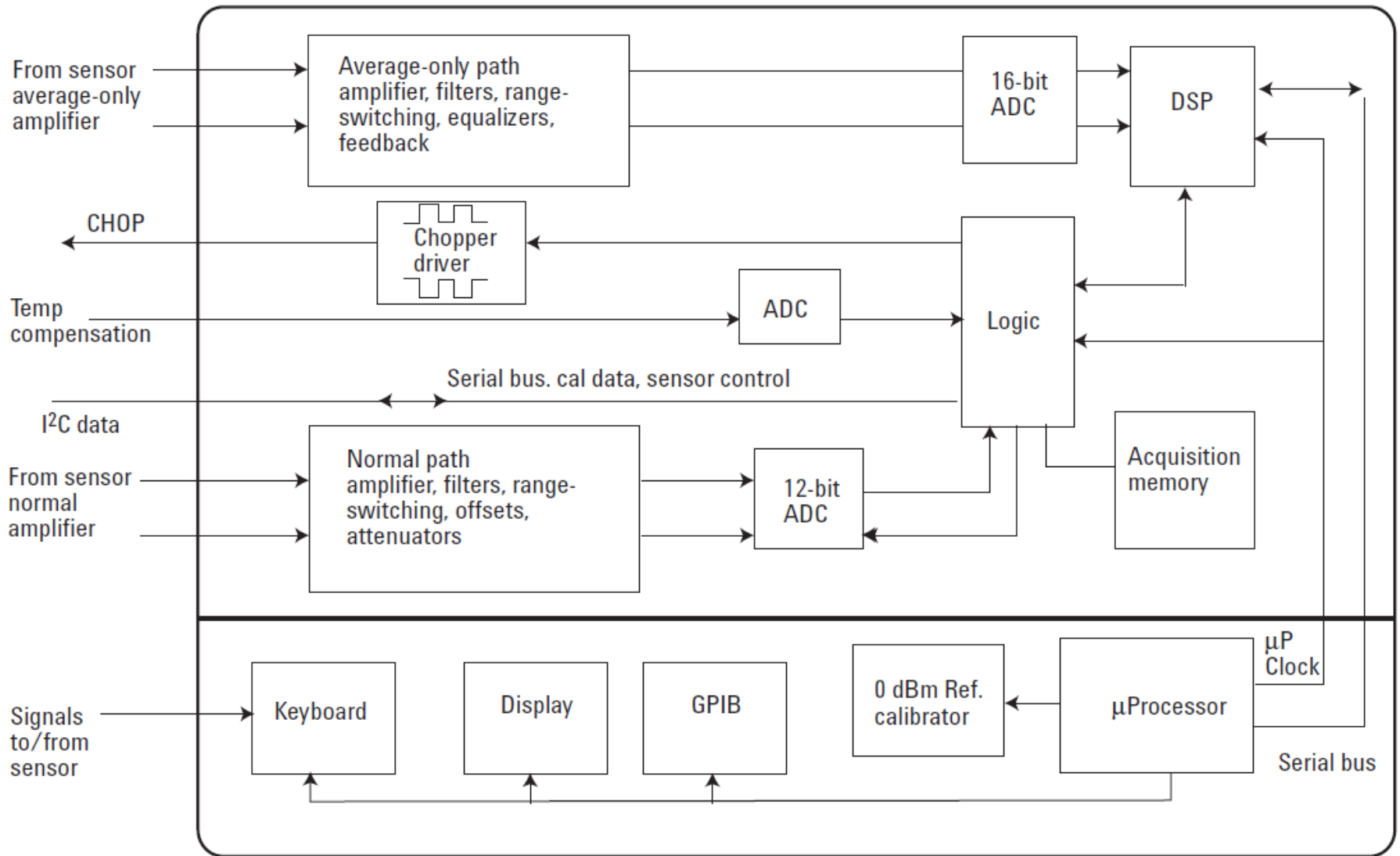
# Peak and average power sensing



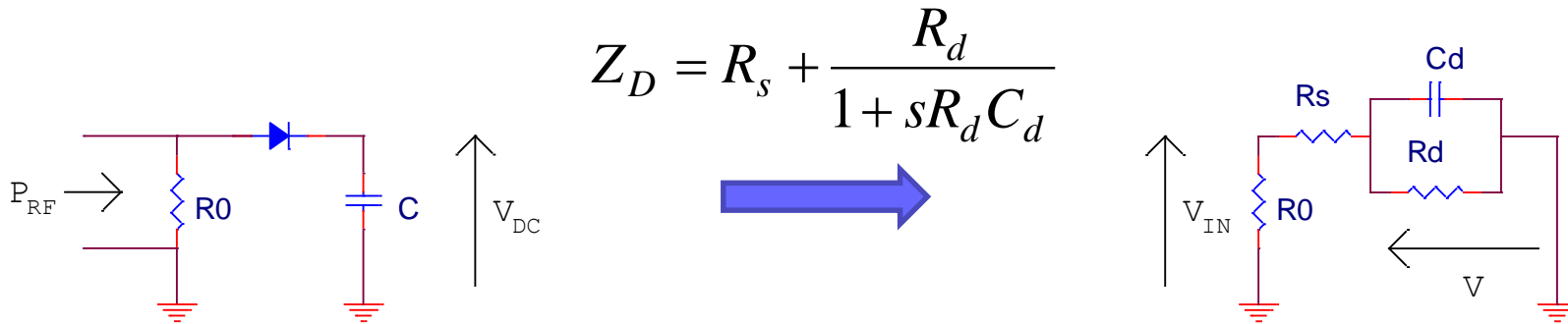
Sensor model	Modulation bandwidth / Max. peak power dynamic range			
	High	Medium	Low	Off
6 GHz/18 GHz				
E9321A/E9325A	300 kHz/-42 to +20 dBm	100 kHz/-43 to +20 dBm	30 kHz/-45 to +20 dBm	-40 dBm to +20 dBm
E9322A/E9326A	1.5 MHz/-37 to +20 dBm	300 kHz/-38 to +20 dBm	100 kHz/-39 to +20 dBm	-36 dBm to +20 dBm
E9323A/E9327A	5 MHz/-32 to +20 dBm	1.5 MHz/-34 to +20 dBm	300 kHz/-36 to +20 dBm	-32 dBm to +20 dBm



# Peak and average power sensing



# Limits in Frequency



$$Z_D = R_s + \frac{R_d}{1 + sR_d C_d}$$

The voltage on the diode junction ( $V$ ) is

$$V = V_{IN} \frac{R_d}{R_s + R_d} \frac{1}{1 + sR_P C_d}$$

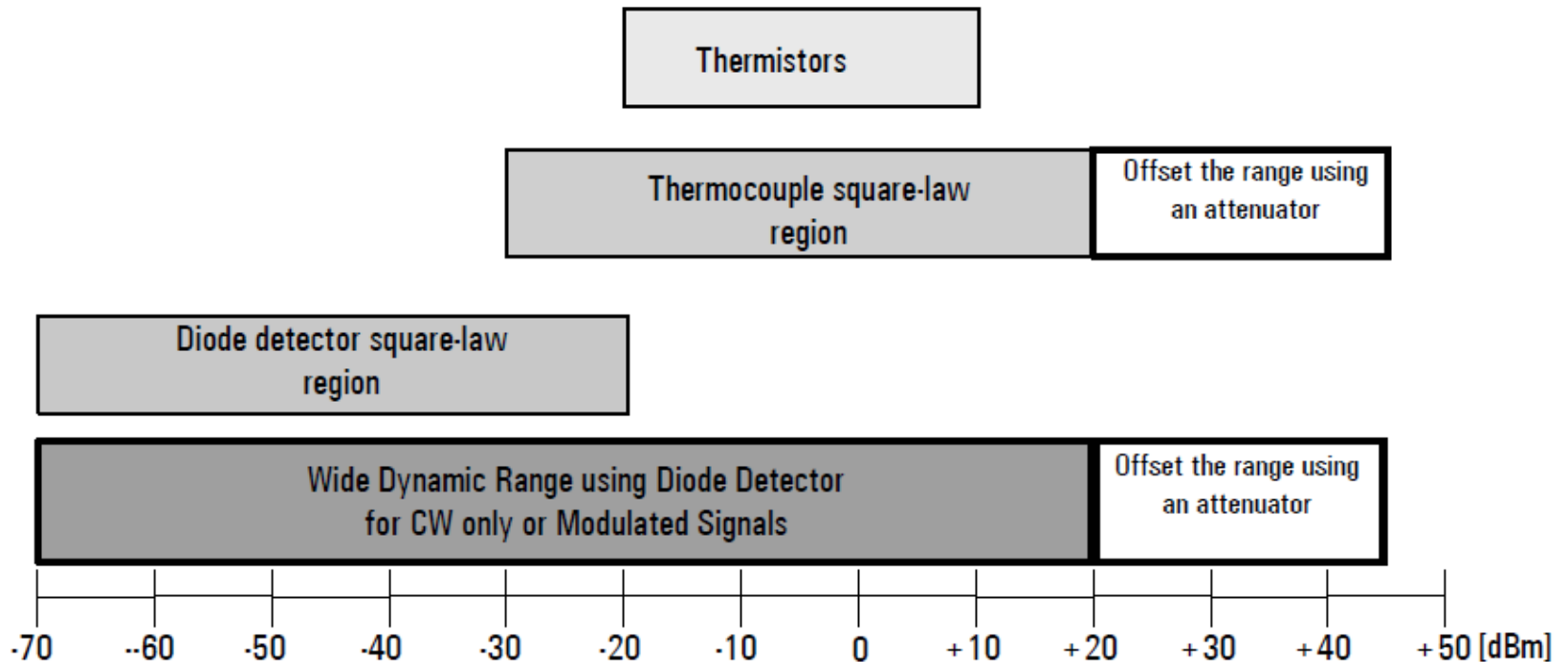
$$R_P = \frac{R_s R_d}{R_s + R_d}$$

The non-linear effect expires with time constant  $\tau = R_P C_d$  BUT the sensor is no more matched before!! (When the diode impedance is close to  $R_0$ )

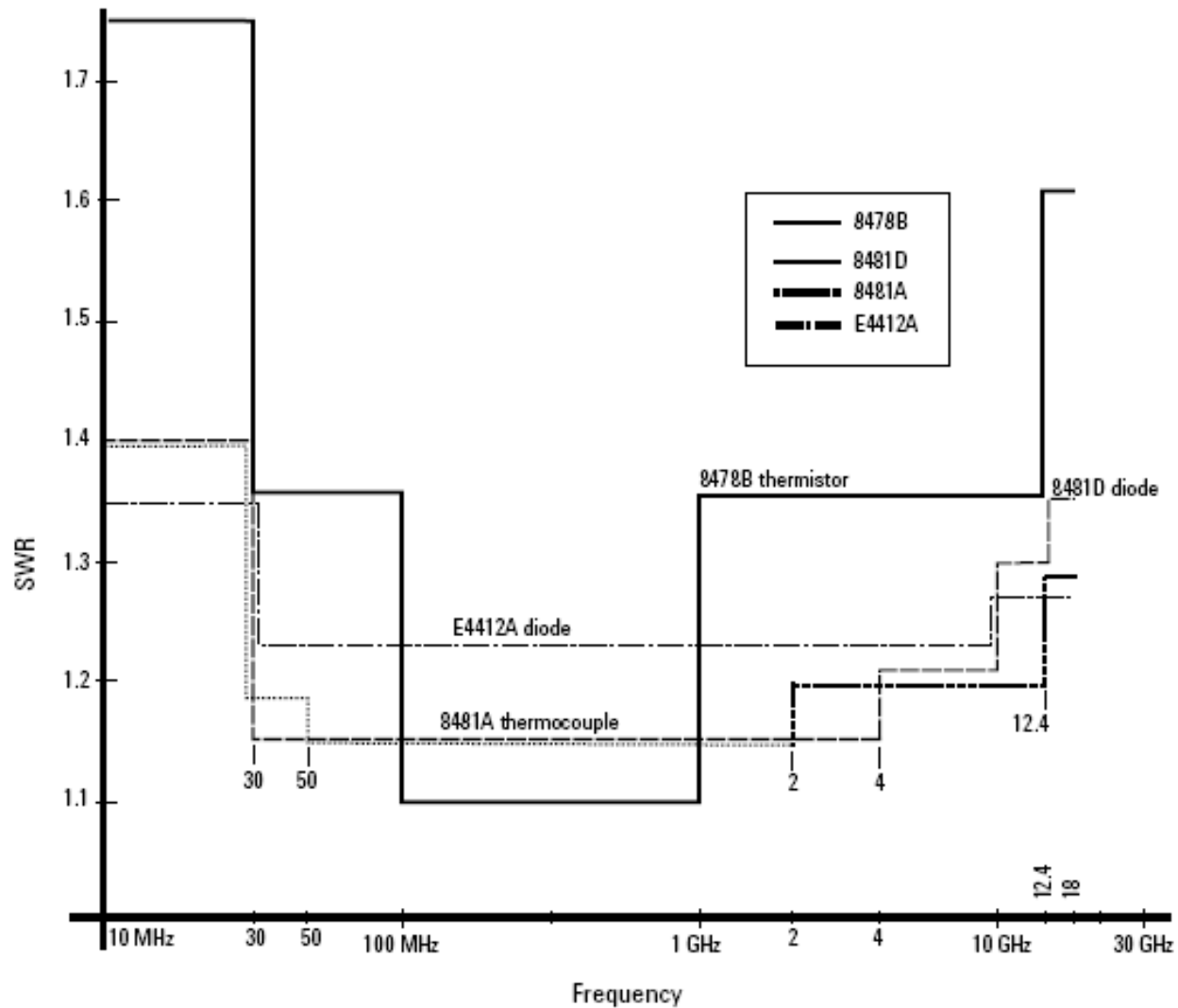
$$Z_D = R_s + \frac{R_d}{1 + j\omega R_d C_d} \cong \frac{R_d}{1 + j\omega R_d C_d} \cong \frac{1}{j\omega C_d}$$

Example: for  $C_d = 0.1$  pF,  $|Z_D| \sim 100\Omega$  at  $f \cong 16$  GHz

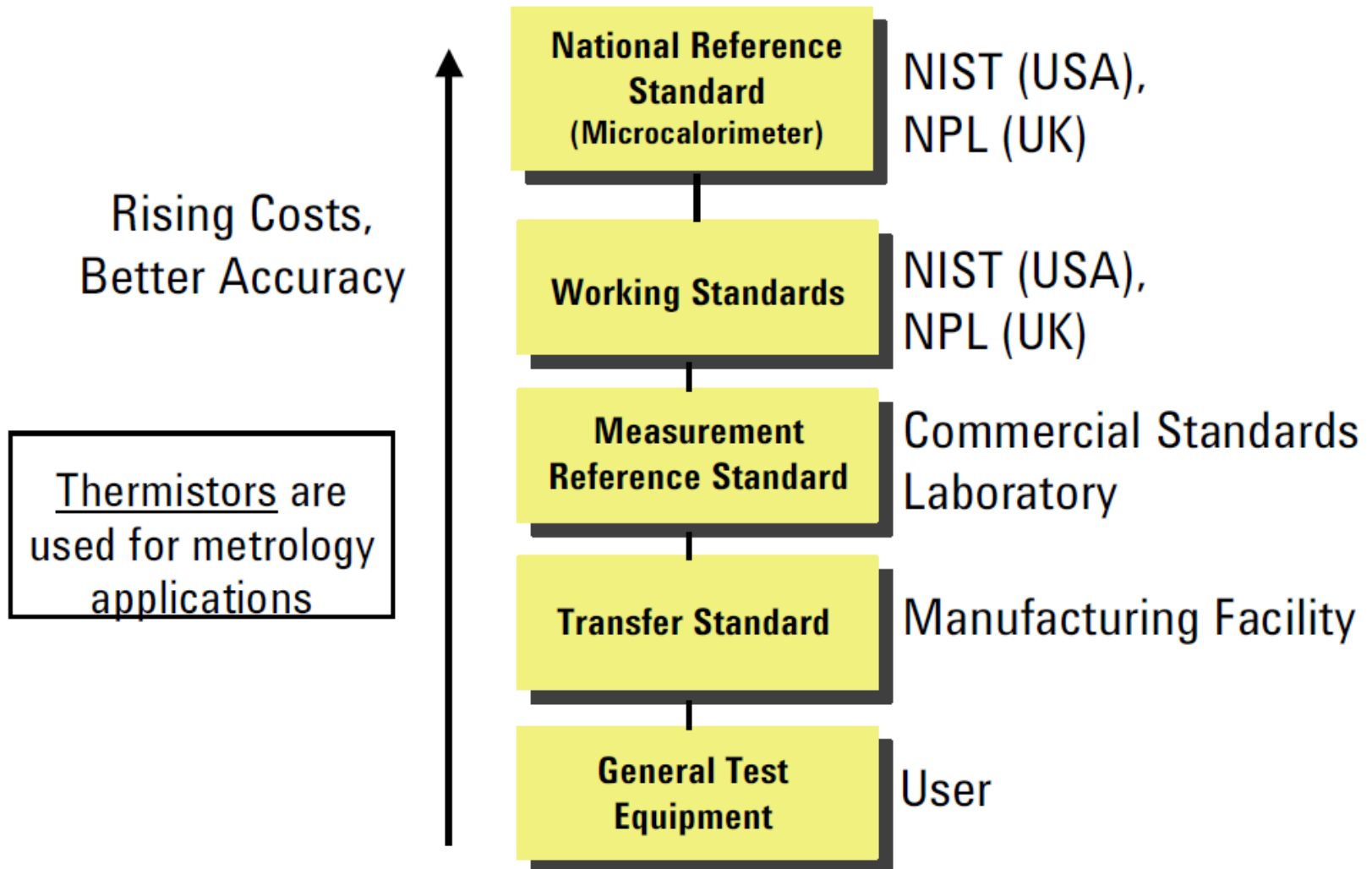
# Power ranges of different sensors



# Mismatch of different power sensors



# The Chain of Power Traceability



# Bolometers (synthesis)

- Coaxial and Waveguide mounts available on the market:
  - Coaxial: 1 MHz to 18 GHz
  - Waveguide: 2.6–200 GHz
- Operate with DC substitution (closed-loop operation)
- Advantages (+) and Disadvantages (–):
  - + Very good long-term stability
  - + Fundamentally very linear
  - Power range: 10  $\mu$ W to 10 mW (30 dB range)
  - High VRC at high frequencies (especially waveguide)
  - Older technology
  - Slow response time
  - Only measure average power
  - Poor dynamic range

# Thermocouples (synthesis)

- Coaxial and waveguide sensors easily available on the market:
  - Coaxial: DC to 50 GHz
  - Waveguide: 8–110 GHz (limited supply outside these frequencies)
- Power range: 1  $\mu$ W to 100 mW (50 dB range)
- Advantages (+) and disadvantages (–):
  - + Good long-term stability
  - + Reasonably linear
  - + Generally lower VRC than thermistor mounts
  - + Easily integrated into automatic systems
  - Often require a reference source
  - Only measure average power

# Diode sensors (synthesis)

- Coaxial sensors easily available in range: 0.1 MHz to 50 GHz
- Power range: 1 nW to 100 mW (90 dB)
- Advantages (+) and disadvantages (–):
  - + Good long-term stability
  - + Reasonably linear at low levels
  - + Generally lower VRC than thermistor mounts
  - + Easily integrated into automatic systems
  - + Fast response allowing envelope power to be tracked
  - + High dynamic range
  - Require a reference source
  - Poor linearity at higher levels
  - Can be inaccurate for modulated and distorted signals



# Diode sensor example

## A Level Detector Design for Dual-Band GSM-PCS Handsets



APN1014

### Introduction

Schottky diode detectors are commonly used as amplitude demodulators and level detectors in wireless and other RF and microwave signal processors. Detector designs are simple to realize using low cost, plastic packaged, silicon Schottky diodes. Figure 1 shows a simple conceptual design.

In this application note we will review detector fundamentals and show the performance of a broadband detector that terminates a 50  $\Omega$  transmission line. Finally, a design for a level detector is presented for use in a dual band GSM-PCS handset. This application uses Alpha's SMS7630 Zero Bias Detector (ZBD) Schottky diode.

### Schottky Detector Fundamentals

#### Schottky Equation

Schottky diode detector operation is based on the equation that characterizes the current-voltage relationship in a diode junction, as shown:

$$I = I_{SAT} \left( e^{\frac{q(V - IR_S)}{nKt}} - 1 \right)$$

Where: n = ideality factor (typically 1.0)

K = Boltzmann's constant, 1.38044 X10<sup>-23</sup> (joule/Kelvin)

q = electronic charge, 1.60206X10<sup>-19</sup> (coulombs)

t = temperature (Kelvin)

R<sub>S</sub> = series resistance ( $\Omega$ )

I<sub>SAT</sub> = saturation current

# Diode sensor example

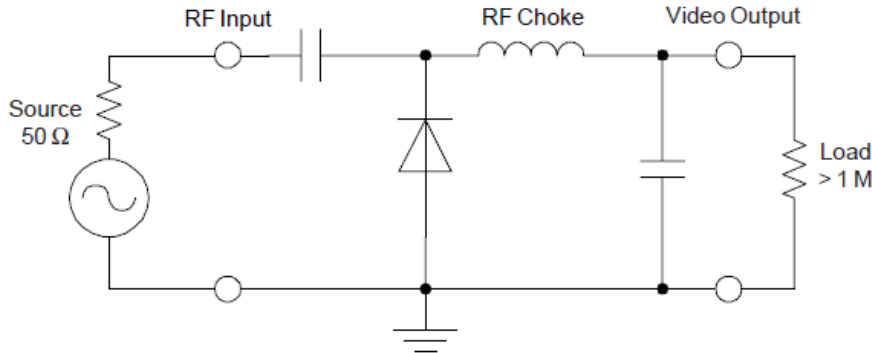


Figure 1. Conceptual Video Detector Circuit

## The Zero Bias Detector (ZBD)

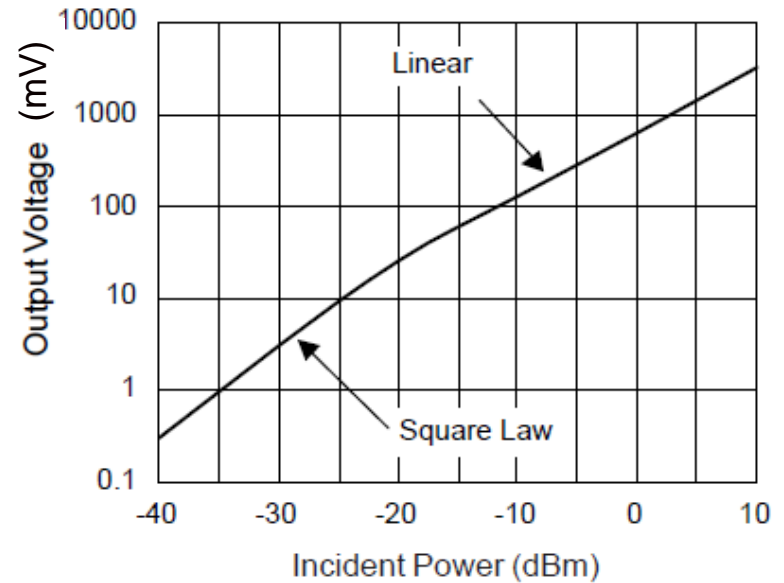
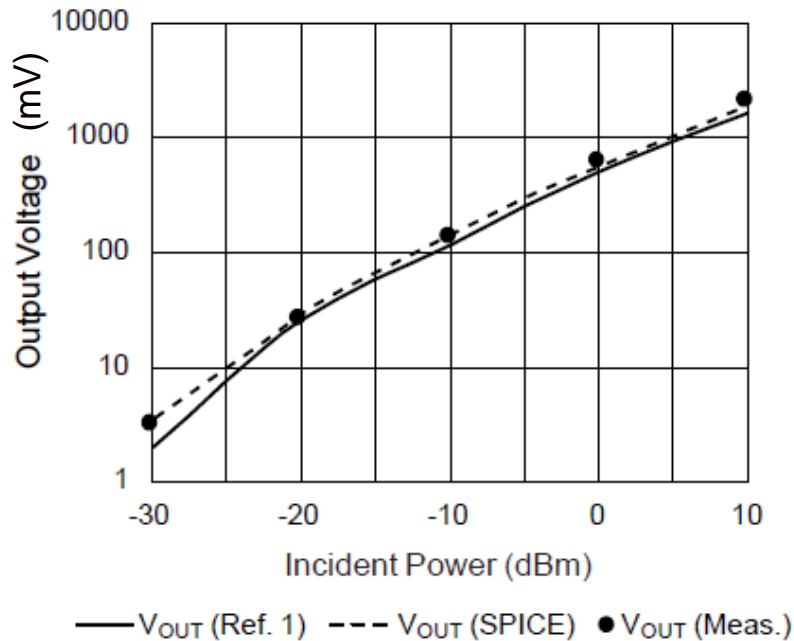


Figure 2. Square Law and Linear Regions



# Diode sensor example

Parameter	Description	Unit	SMS7630 & Default	SMS1546 & Default
IS	Saturation current	A	5E-6	3E-7
R <sub>S</sub>	Series resistance	Ω	30	4
N	Emission coefficient (Not used)	-	1.05	1.04
TT	Transit time (Not used)	S	1E-11	1E-11
C <sub>JO</sub>	Zero-bias junction capacitance (Not used)	F	1.4E-13	3.8E-13
V <sub>J</sub>	Junction potential (Not used)	V	0.34	0.51
M	Grading coefficient (Not used)	-	0.4	0.36
E <sub>G</sub>	Energy gap (with XTI, helps define the dependence of IS on temperature)	EV	0.69	0.69
XTI	Saturation current temperature exponent (with E <sub>G</sub> , helps define the dependence of IS on temperature)	-	2	2
KF	Flicker-noise coefficient (Not used)	-	0	0
AF	Flicker-noise exponent (Not used)	-	1	1
FC	Forward-bias depletion capacitance coefficient (Not used)	-	0.5	0.5
B <sub>V</sub>	Reverse breakdown voltage (Not used)	V	2	2.5
I <sub>BV</sub>	Current at reverse breakdown voltage (Not used)	A	1e-4	1e-5
ISR	Recombination current parameter (Not used)	A	0	0
NR	Emission coefficient for ISR (Not used)	-	2	2
IKF	High-injection knee current (Not used)	A	Infinity	Infinity
NBV	Reverse breakdown ideality factor (Not used)	-	1	1
I <sub>BVL</sub>	Low-level reverse breakdown knee current (Not used)	A	0	0
NBVL	Low-level reverse breakdown ideality factor (Not used)	-	1	1
T <sub>NOM</sub>	Nominal ambient temperature at which these model parameters were derived	°C	27	27
FFE	Flicker-noise frequency exponent (Not used)		1	1

Table 1. Silicon PN Diode Values in Libra IV Assumed for SMS7630 and SMS1546 Models

# Diode sensor example

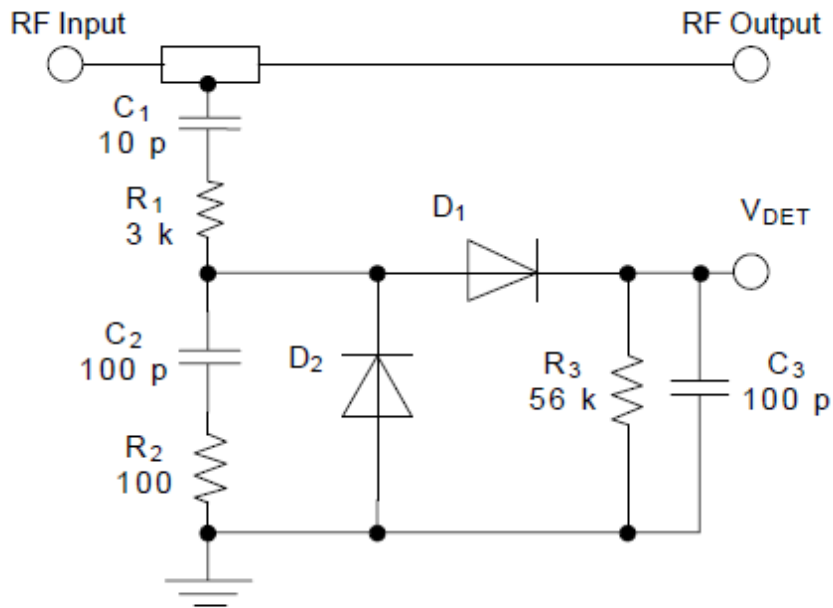


Figure 5. Level Detector Circuit Diagram

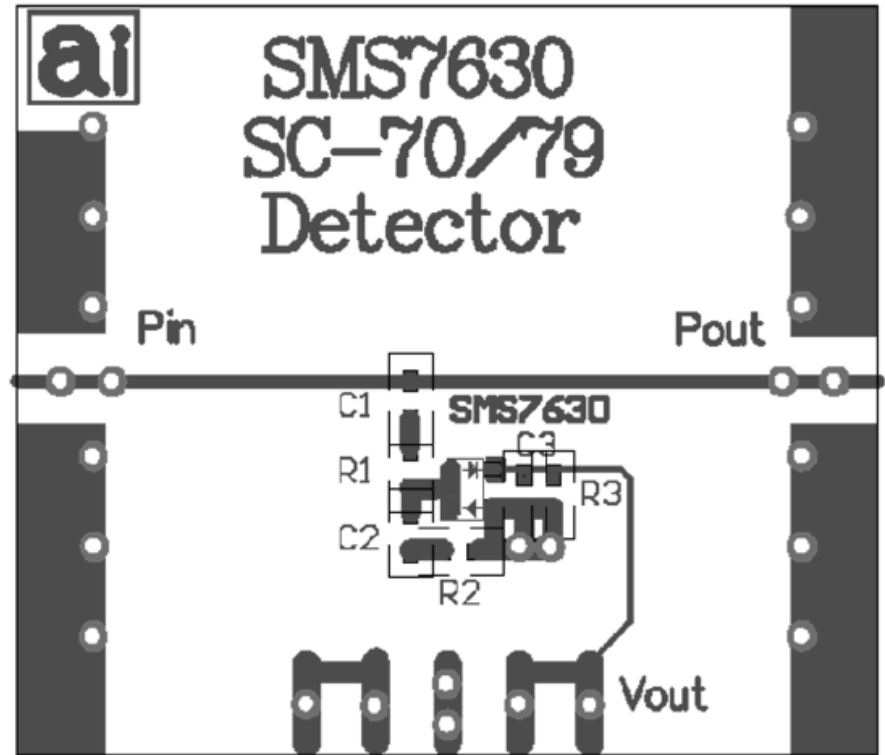


Figure 7. Detector PCB Layout

# Diode sensor example

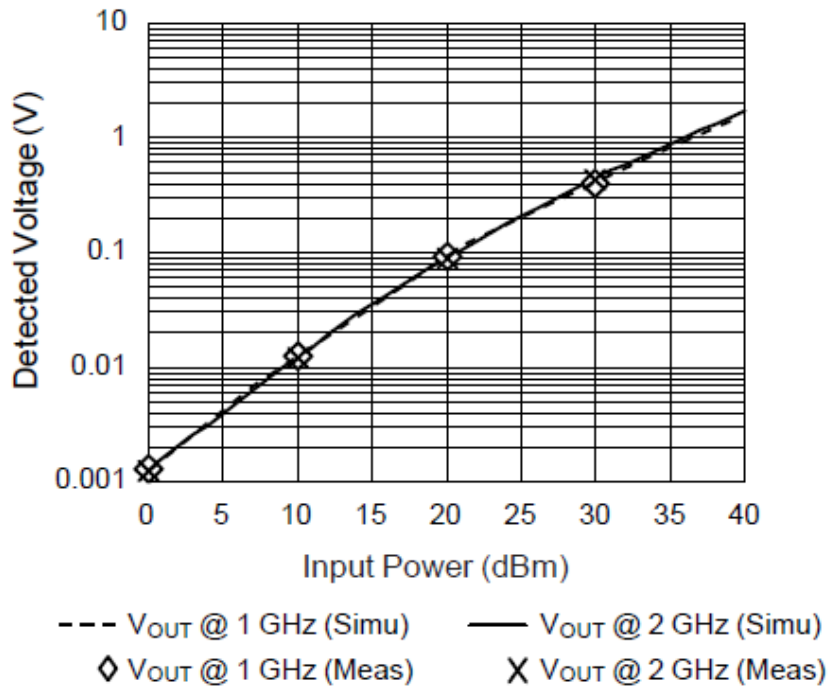


Figure 8. Detector Output Voltage vs. Input Power

Input Power	$V_{OUT}$	$V_{OUT}$	$V_{OUT}$	$V_{OUT}$	$V_{OUT}$	$V_{OUT}$
	800 MHz	1 GHz	1.2 GHz	1.8 GHz	2.0 GHz	2.2 GHz
-10 dBm	0.131	0.129	0.128	0.122	0.118	0.112
0 dBm	1.24	1.23	1.22	1.21	1.18	1.13
5 dBm	4.15	4.13	4.11	3.88	3.84	3.12
10 dBm	12.23	12.21	11.99	11.91	11.53	11.39
15 dBm	34.81	34.62	34.33	33.77	33.65	33.53
20 dBm	91.38	91.36	91.35	88.86	86.51	83.91
30 dBm	422.65	422.61	422.15	421.38	419.38	405.31

Table 3. Detector Frequency Response

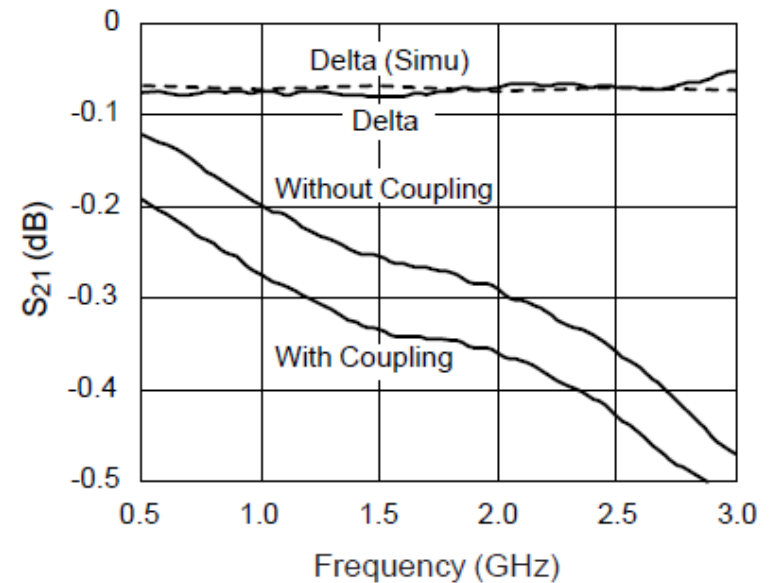


Figure 9. Detector Loss vs. Frequency